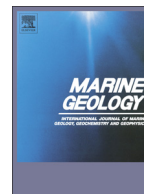




Contents lists available at ScienceDirect

Marine Geology

journal homepage: [www.elsevier.com/locate/margeo](http://www.elsevier.com/locate/margeo)

## Storm-driven cyclic beach morphodynamics of a mixed sand and gravel beach along the Mid-Atlantic Coast, USA

Tiffany M. Roberts <sup>a,\*</sup>, Ping Wang <sup>b</sup>, Jack A. Puleo <sup>c</sup>

<sup>a</sup> Louisiana State University, Department of Geology & Geophysics, Baton Rouge, LA, USA

<sup>b</sup> University of South Florida, Coastal Research Laboratory, Department of Geology, Tampa, FL, USA

<sup>c</sup> University of Delaware, Center for Applied Coastal Research, Department of Civil and Environmental Engineering, Newark, DE, USA

### ARTICLE INFO

#### Article history:

Received 12 June 2012

Received in revised form 29 July 2013

Accepted 4 August 2013

Available online xxxx

Communicated by J.T. Wells

#### Keywords:

beach cycles

storm-impact

storm deposits

post-storm recovery

mixed beach morphology

sandbar

Nor'Ida

Delaware

### ABSTRACT

The morphodynamics of a mixed sand and gravel beach in Delaware were investigated based on 18 almost monthly beach-profile surveys at 46 locations from 2009 to 2011, 60 sediment cores, and 550 surface sediment samples collected at various alongshore and cross-shore transects. Three different atmospheric disturbances occurred within a 3-month window during the study period: 1) a distal hurricane, 2) an energetic winter storm, and 3) "Nor'Ida", a long-lasting and extremely energetic event resulting from the collision of a hurricane and winter storm. The storm-induced beach changes and post-storm recovery following each of the three storms are evaluated. A distinctive beach cycle was identified consisting of a built-up berm profile and depleted nearly-planar storm profile. The time-scale of the beach cycle relates to the frequency and intensity of storm impact and duration of inter-storm recovery instead of simple seasonality. The initiation of post-storm recovery occurs during the subsiding phase of the storm, attributable to the reduction in wave height and steepness transitioning to accretionary swells. The sediment characteristics of the storm deposit associated with Nor'Ida demonstrated substantial cross-shore variation ranging from sandy-gravel and gravelly-sand within the storm swash zone (near the pre-storm dune edge) to well-sorted medium to coarse sand seaward of the storm swash zone. Storm deposits along mixed sand and gravel beaches demonstrate a variety of sedimentological characteristics. In addition, the studied beaches lacked a sandbar under all wave conditions. A new beach cycle model is proposed for the non-barred mixed sand and gravel beach.

© 2013 Elsevier B.V. All rights reserved.

### 1. Introduction

Understanding beach morphodynamics at myriad temporal and spatial scales is important for both scientific inquiry and beach management practices. Although geographically variable and influenced by regionally-specific geologic and oceanographic processes, site-specific beach change studies at multiple temporal and spatial scales aid in the understanding and generalization of beach morphodynamics (Dean, 1977; Bodge, 1992; Inman et al., 1993; Larson and Kraus, 1994; Larson et al., 1999; Ruggiero et al., 2005). Often, the generalization of beach morphodynamics is placed into the context of beach cycles, typically with a seasonal periodicity. Shepard (1950) and Bascom (1953) were among the first to document different beach profile shapes during the winter and summer seasons. The varying profile shapes are interpreted to be controlled by the generalized seasonality in wave climate. During the winter season, frequent winter storms tend to erode the subaerial beach

and transport the sediment offshore, depositing in the form of a sandbar. During the summer season, the frequent swell-type waves tend to move the sandbar onshore, subsequently attaching to and widening the subaerial beach (Komar, 1998).

Numerous studies have been conducted on the morphodynamics of nearshore bars on sandy beaches (Wright and Short, 1984; Kraus and Larson, 1988; Larson et al., 1988; Kraus et al., 1992; Ruessink and Kroon, 1994; Lee et al., 1998; Plant et al., 1999; Morton and Sallenger, 2003). One of the well-documented mechanisms for bar formation is related to high, steep storm waves. The cross-shore profile responds to storms by forming a sandbar from eroded berm sediment or the offshore migration of an already existent sandbar (Holman and Bowen, 1982; Sallenger et al., 1985; Boczar-Karakiewicz and Davidson-Arnott, 1987; Larson and Kraus, 1989; Holman and Sallenger, 1993; Kriebel and Dean, 1993; Gallagher et al., 1998; Hoefel and Elgar, 2003). Hoefel and Elgar (2003) showed one mechanism for offshore sandbar migration is the breaking of large storm waves over the sandbar driving a strong offshore-directed undertow reaching a maximum just over the bar crest. Gallagher et al. (1998) modeled offshore sandbar migration using an energetics-type sediment transport formulation. In the summer season, the common occurrence of long-period swells tends to cause the sandbar to migrate onshore, attach to the beach, and build-up the berm.

\* Corresponding author. Tel.: +1 225 578 2801.

E-mail address: [tiffanyroberts@lsu.edu](mailto:tiffanyroberts@lsu.edu) (T.M. Roberts).

The process of onshore bar migration tends to happen over a period of weeks to months, occurring slower as compared to the often single event-driven (i.e., storm induced) offshore migration (Greenwood, 2005). The process driving onshore bar migration is not as well-quantified as offshore migration.

The above studies were mostly focused on sandy beaches. Although the influence of cross-shore grain size variations on the beach profile is acknowledged, little is known about the morphodynamic influence of the large grain-size variation associated with a mixed sand-gravel (MSG) beach. The morphodynamics of MSG beaches exhibit somewhat different transport mechanisms and morphologic characteristics compared to sandy beaches (Mason and Coates, 2001; Pontee et al., 2004; Horn and Li, 2006; Horn and Walton, 2007; Karunaathna et al., 2012). Due to the permeable nature of gravel-sized sediment, infiltration and interaction with groundwater can influence sediment transport processes on MSG beaches (Turner and Masselink, 1998; Mason and Coates, 2001; Horn and Li, 2006). Depending on the spatial distribution of sediment at varying temporal scales, the content ratio of gravel and sand will also affect sediment transport processes and the resulting morphology (Pontee et al., 2004; Austin and Masselink, 2006; Masselink and Puleo, 2006).

The morphology of MSG beaches tends to vary due to the broad range of processes influencing transport, as well as the large variations of sand/gravel ratio. For example, in New Zealand, the primary morphologic characteristic of a MSG beach was a steep migratory break-point step modulated by tidal water level fluctuations and the absence of an offshore sandbar (Ivamy and Kench, 2006). Horn and Walton (2007) identified another type of MSG beach in the UK, where the reflective upper beach is composed of mixed sand and gravel, with a flat dissipative sandy low-tide terrace. Horn and Walton (2007) examined temporal changes in sand and gravel distribution patterns associated with a beach nourishment consisting of bi-modal sediment. Most of the MSG beach studies focus primarily on the intertidal and supratidal beach regions, whereas corresponding morphology in the direct offshore regions is less well-documented (Carter and Orford, 1993; Jennings and Shulmeister, 2002; Neal et al., 2002).

Morphological and sedimentological impacts of storms have been the topic of numerous studies on sandy beaches, typically along barrier islands (Morton et al., 1994; Forbes et al., 2004; Hill et al., 2004; Stone et al., 2004; Ruggiero et al., 2005; Wang et al., 2006; Claudino-Sales et al., 2008, 2010). Most of these studies focus primarily on large storm-induced cross-shore profile changes with less attention focused on the immediate post-storm recovery (Morton et al., 1994; Stone et al., 2004; Ruggiero et al., 2005; Wang et al., 2006; Houser and Hamilton, 2009). Wang et al. (2006) found that the berm crest elevation and foreshore slope recovered rapidly (within a month) following the impact of Hurricane Ivan along the northwest coast of Florida. Short-term recovery (1–2 years) of the beach width and dune field was minimal. Ruggiero et al. (2005) emphasized the importance of improved understanding of beach behavior associated with storms on multiple scales, including inter-annual (e.g., seasonality), decadal (e.g., El Niño and La Niña cycles), and long-term scales associated with climate change (e.g., sea-level changes). Some studies conducted along MSG beaches have documented morphodynamic responses both similar to and different from sandy beaches (Neal et al., 2002; Pontee et al., 2004; Orford and Anthony, 2011). Pontee et al. (2004) identified that although the profile response to tidal fluctuations, wave conditions, and accretion via ridge welding of MSG beaches is similar to sandy beaches, the morphology of the lower foreshore often differs between the two. Pontee et al. (2004) emphasized that rapid changes in sediment texture and short term variability of profiles in response to storms are different for MSG beaches as compared to sandy beaches.

The morphodynamics and sedimentary characteristics of a MSG beach in Delaware, USA are investigated based on 18 beach profile surveys at 46 locations (total of 740 beach profiles) extending to over 10 m water depth surveyed almost monthly from 2009 to 2011, 550 surface sediment

samples, and 60 sediment cores. Three different atmospheric disturbances occurred within a 3-month window during the study period: 1) a distal hurricane, 2) an energetic winter storm, and 3) “Nor’Ida”, a long-lasting and extremely energetic event resulting from the collision of a hurricane and winter storm. These energetic events provided a unique opportunity to study the morphodynamics of a MSG beach, including: 1) beach–nearshore profile response to storms with different oceanographic and initial-profile characteristics; 2) sedimentological characteristics of storm deposits; and 3) post-storm recovery. It is hypothesized that selective transport and deposition associated with a wide range in sediment grain size and under various wave energy conditions provide a specific set of morphological and sedimentological characteristics of MSG beaches. Specifically, this study aims at documenting a large range of parameters associated with a MSG beach, including the beach–nearshore profile evolution and associated spatiotemporal scales as well as the horizontal and vertical distribution of sediment characteristics controlled by selective transport under storm and calm-weather conditions.

## 2. Study area

Delaware is located on the United States mid-Atlantic seaboard (Fig. 1), just south of the southern-most extent of the Laurentide icesheet that covered much of North America 17,000 years ago (Lemcke and Nelson, 2004). Delaware’s coastal geology reflects the post-Wisconsinan transgression and glacial outwash that resulted in landward shoreline migration from its location on the edge of the continental shelf 120 km east of the present-day location. The post-glacial transgression resulted in the infilling of valleys with swamp, stream, marsh, and lagoonal deposits, later overlain by nearshore and offshore sediments, and the formation of barrier islands (UDel/DE SGP, 2004). Offshore sediments are primarily composed of fine to coarse sand and sandy gravel to gravel, characteristic of glacial outwash (Ramsey, 1999). Using over 55 years of data from beach sand samples, Ramsey (1999) determined the native composite of sediment in Delaware to be between 1.5 and 0.5  $\phi$  (0.35 to 0.71 mm) in mean grain size with a standard deviation of 0.5  $\phi$ , classified as well-sorted medium sand (Wentworth, 1922). Considerable variation in surface and subsurface sediments results from post-transgression sediment reworking, with lagoonal deposits overlain by silt to very coarse sand-gravel in the offshore and fine sand to pebbles in the nearshore (McKenna and Ramsey, 2002). Recent large-scale beach nourishments using sand borrowed from the offshore glacial outwash deposits has resulted in a gradual coarsening of beach sediment, towards a more mixed sand and gravel beach (McKenna and Ramsey, 2002).

The roughly north–south trending 40 km-long Delaware coast is bound to the north by Delaware Bay, terminating as a northward accreting spit known as Cape Henlopen (Fig. 1A). No specific geographic feature bounds Delaware to the south, although the state border terminates at roughly the eastern-most apex of the large broad headland of the Delmarva Peninsula (comprised of Delaware, Maryland, and Virginia) that has been identified as a nodal point in longshore sediment transport (Dalrymple and Mann, 1986; Puleo, 2010). The littoral drift along Delaware is interrupted by the structured Indian River Inlet. Based on sediment volume change on the ebb delta, Lanan and Dalrymple (1977) determined the net northward longshore sediment transport rate at Indian River Inlet to be approximately 100,000 m<sup>3</sup>/yr. Based on hindcast wave data, Puleo (2010) estimated the potential net northward longshore sediment transport to be 370,000 m<sup>3</sup>/yr. Gross transport rates reportedly vary between 535,000 and 688,000 m<sup>3</sup>/yr (USACE, 1996). Large seasonal shifts in Delaware beach morphology occur, with cyclical changes in berm shape and elevation (Dubois, 1988) and shoreline position changes of 75 m (Ozkan-Haller and Brundidge, 2007).

Winds vary seasonally, with prevailing northwesterly winds during the winter and southwesterly winds during the summer. The strongest winds tend to coincide with the passage of winter northeasters (nor’easters), with the easterly component of wind directed onshore.

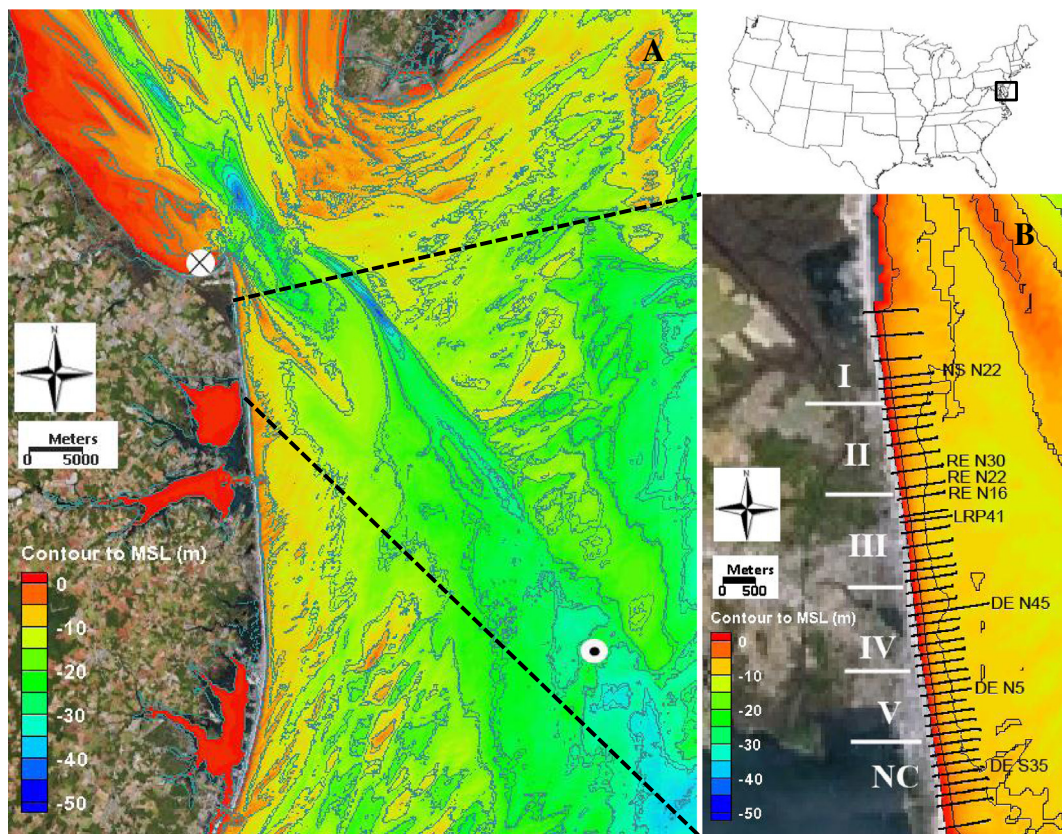


**Fig. 1.** Study area map of the Delaware coast. The general US location and bathymetry is shown in the upper right. A) The offshore bathymetry was obtained from the Coastal Relief Model and combined with the bathymetric data collected for this study, contours relative to Mean Sea Level (MSL). The location of the tidal gauge is shown by a circle with an "x". The NDBC wave buoy location is shown by a circle with a black dot. B) A close-up of the study area is shown with the locations of the beach profiles (a few labeled for reference) and profile-averaged regions.

Recognizing the importance of northeasters to the morphodynamics of the US Atlantic coast, Dolan and Davis (1992) developed a northeast storm intensity scale based on the so-called storm power, which is defined as the product of the storm duration and square of maximum significant wave height. Onshore-directed winds associated with northeasters can also induce elevated water levels. Winter storms tend to last over several tidal cycles (Herrington and Miller, 2010; Munger and Kraus, 2010) compared to tropical storms that are less frequent and typically of shorter duration.

Tides along the open-coast beaches are semi-diurnal with a mean tidal range of 1.2 m. It is worth noting that a portion of the Delaware coast is likely influenced by the shadowing effect of the protruding New Jersey landmass (north of Delaware Bay), altering the propagation patterns of northerly-approaching wind and waves (Fig. 1A). The average significant wave height and dominant wave period obtained from an offshore wave buoy (NDBC 44009) between 2008 and 2011 were 1.27 m and 7.6 s respectively, with a maximum wave height of 8.11 m (measured during Nor'Ida) and a maximum wave period of 19 s (similar to the peak period of the Hurricane Bill-induced swell, as discussed in the following) measured during the four-year period. Notably, high wave-energy conditions in the summer are much less common than those during the winter, due to the rarity of tropical storm impacts to the study area. During the 4-year period between 2008 and 2011, the 2009–2010 winter was the most energetic (Fig. 2).

### 3. Methodology

Beach-profile data were collected by the Delaware Department of Natural Resources and Environmental Control (DNREC) at 46 alongshore locations spaced approximately 200 m apart. Beach profiles used in this

study (Figs. 1B and 3) were surveyed nearly monthly at these locations from July 2009 to October 2011 (total of 740). Beach-profile data were collected using a Real-Time Kinematic Global Positioning System (RTK-GPS) for both the subaerial (beach) and subaqueous (offshore) areas. The RTK-GPS was mounted on a survey rod and surveyed to approximately 1 m. The offshore profile was surveyed using a vessel-mounted synchronized RTK-GPS and precision echo-sounder system. The two sections of the profiles overlapped with the combined profiles used in this study. Elevation data are referenced to NAVD88 (0 m NAVD88 is 0.1 m above Mean Sea Level (MSL) in this area). Profiles extend approximately 1 km offshore to at least 10 m water depth, or beyond the depth of closure in the study area (Garringa and Dalrymple, 2002; Ozkan-Haller and Brundidge, 2007; Figus and Kobayashi, 2008). Surveying the set of cross-shore profiles spanned several tidal cycles. Therefore, beach profile changes associated with tidal variations could not be resolved.

Alongshore and temporal averaging of time-series beach profiles was conducted in order to obtain a representative profile. Each profile was surveyed approximately 16–18 times during the 2-year study period. An average of all surveys at each specific profile location was obtained so that a total of 46 mean profiles were established (for each profile location). Each average profile was then shifted such that the origin of the cross-shore coordinate, i.e., 0 m distance, corresponds to 0 m NAVD88 for spatial averaging. Five regions were defined, for the convenience of discussion (Fig. 1B), to minimize the influence of regional alongshore variations in the offshore bathymetry on the alongshore spatial averaging of the profiles (Fig. 1A). Each region has 6 to 8 time-averaged profiles. The profiles at the south end of the study area were not included in the analysis of the averaged profiles, as this section of beach was nourished during the study period, but included in the regional analysis of beach morphology changes.

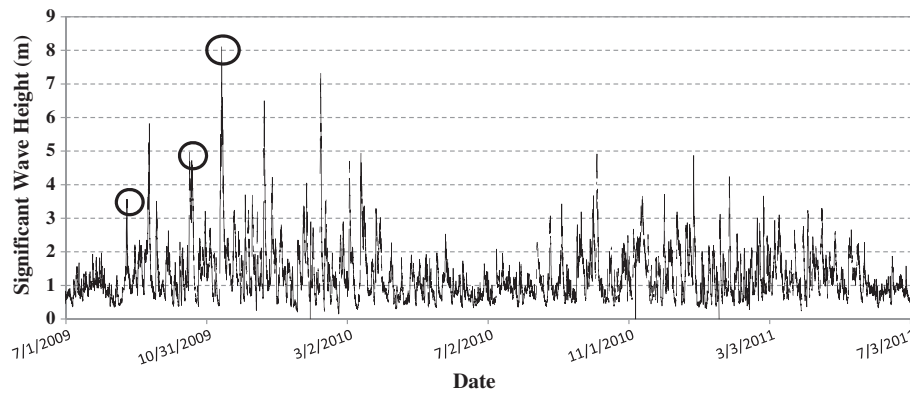


Fig. 2. Significant wave height during the study period from 2009 to 2011 measured at the NDBC 44009 buoy. The peak wave heights associated with the three storms discussed are indicated by circles.

One of the most energetic storm events on record for this region impacted the northeastern US coast (Grosskopf and Bass, 2010; Herrington and Miller, 2010) during the first year of the study. The return interval for this storm was designated as 45 to 90 years based on beach erosion potential, evaluated by Munger and Kraus (2010). However, Hurricanes Irene in 2011 and Sandy in 2012, after our study period, may have some influence on the return period estimation. This storm resulted from remnants of Hurricane Ida and a nor'easter that collided off the Atlantic

coast in November 2009, and has been colloquially referred to as the “Friday the 13th storm” or “Nor’Ida”. In the following, this storm is referred to as “Nor’Ida”.

Nor’Ida had a tremendous impact to the study area and is examined here in comparison to two other significant meteorological events that occurred three months and one month, respectively, prior to Nor’Ida: the distal passage of Hurricane Bill in August 2009 and the first significant nor’easter of the 2009 winter season in October. Water-level measurements were obtained from the National Oceanic and Atmospheric Administration buoy, NOAA 8557380, located just west of Cape Henlopen in Delaware Bay in Lewes, Delaware (circle with x in Fig. 1A). Significant wave height and dominant wave period were measured hourly at an offshore buoy, (National Data Buoy Center; NDBC 44009, circle with black dot in Fig. 1B), located roughly 30 km offshore from the Delaware–Maryland state border line in 28 m of water. Wave direction was not reported by the NDBC 44009 during the study period. Wave direction was instead obtained using WAVEWATCH III data (NOAA WAVEWATCH III).

The CMS-Wave model was used (Lin et al., 2008) to investigate the influence of the complicated bathymetry in the greater study area on the nearshore wave field, especially during the three storms. The bathymetry in the greater study area was extracted from the Coastal Relief Model (NOAA CRM). Within the study area (Fig. 1B), the CRM bathymetry was updated by the profile survey data. Four schematic wave runs were conducted based on statistical wave parameters obtained from NDBC 44009 and WAVEWATCH III, including 1) an average wave condition, 2) an averaged swell condition associated with the distal passage of Hurricane Bill, 3) an averaged wave condition during the October winter storm, and 4) an averaged wave condition during the Nor’Ida storm. The averaging scheme is discussed in the Results section.

Surface and subsurface sediment samples were collected to examine alongshore and cross-shore variations in sediment characteristics along the MSG beach, as well as changes associated with storm impacts and post-storm recovery (Fig. 3). Three different sampling schemes were adopted: 1) storm-related, 2) seasonal sampling, and 3) calm-weather sampling. Thirty-four sediment cores were obtained over a week-long period associated with the Nor’Ida storm in November 2009. Pre-Nor’Ida and post-Nor’Ida sediment cores were obtained from the backbeach, berm, and swash zone. Core locations were chosen in relation to the observed beach morphology rather than at some constant distance from a fixed benchmark. Sampling in this fashion ensures that comparisons across time are consistent with respect to local morphology. Sediment cores were collected using both vibracore and pound core methods (Wang and Horwitz, 2007).

The sediment sampling, focused in the middle of the study area in regions I, II and III, aims to characterize cross-shore sediment property



Fig. 3. Locations of selected sediment cores (crosses), surface samples (circles), and offshore samples (triangles) in reference to beach profiles (shore-perpendicular lines) discussed in this paper.

variation linked to morphologic features. The temporal sampling is aimed at identifying seasonal and storm-induced sediment property variations. Seasonal surface sediment samples were collected from the top 5 cm of the bed on the backbeach, berm, and swash zone. These samples were obtained bi-annually during the study period, between August 2009 and May 2011. Offshore sediment samples were obtained using a spring-loaded grab-sampler at water depths of approximately 3, 5, and 7 m along nine survey lines. The offshore sediment sampling was conducted during calm weather in the summer of 2010. During this time, additional surface samples were collected within the inner surf zone to document the cross-shore distribution of gravel during calm weather to compare with the gravel distribution observed during Nor'Ida. The three locations included the lower limit of backwash (swash zone near the plunge step), at the shorebreak point (landward-most breaker), and approximately the mid-surf zone. Overall, due to the large seasonal and storm-induced morphology changes, the sediment sampling was based on observed (spatial) and instantaneous (temporal) morphological characteristics, as described above, instead of fixed geographic locations. Photos were also obtained to aid in field observations and data analysis.

## 4. Results

### 4.1. General morphology and sedimentology

The bathymetry in the greater study area is heterogeneous (contours are not shore-parallel) and influenced by the large ebb-tidal delta associated with the Delaware Bay entrance. The primary study area is located landward of this southeast trending ebb delta (Fig. 1A). It is reasonable to assume that the delta has some influence on wave propagation patterns, however the complicated bathymetry associated with the ebb delta is mostly deeper than 10 m and beyond the 7 m closure depth, as determined by previous studies (Garringa and Dalrymple, 2002; Ozkan-Haller and Brundidge, 2007; Figlus and Kobayashi, 2008). The detailed wave dynamics associated with the ebb delta are beyond the scope of this study. A schematic wave propagation modeling (discussed in the following section) was conducted to provide general information on wave field.

Generally the backbeach elevation is about 2 m above NAVD88, which is the typical height of the built-up summer berm. The foreshore between the berm crest (~2 m NAVD88) and about -1 m is steep, with an average slope ranging between 1/20 and 1/10, depending on the beach state. The storm beach profile tends to be gentler. Localized

steepening of the beach slope occurs in the swash zone often in conjunction with the presence of a plunge step, corresponding to the larger grain size present within this region of the profile. Throughout the study area, a laterally extensive dune ridge exists with an average dune crest elevation of approximately 5 m NAVD88, both naturally occurring and anthropogenically constructed.

One of the most distinctive morphological characteristics in the study area is the absence of a nearshore sandbar under all wave conditions (Fig. 4). Time-series of beach profiles shows that eroded berm sediment was transported offshore following winter storms (10/09 and 11/09). However, the offshore-directed sediment transport and deposition did not result in a sandbar morphology, as observed along numerous coasts (Larson and Kraus, 1994; Ruessink and Kroon, 1994; Grunnet et al., 2004; van Duin et al., 2004). The absence of an offshore sandbar is intriguing although not yet explained, and will be discussed in following sections.

Between the berm crest (~2 m above MSL) and about 3 m water depth, all of the average profiles overlay each other with little to no difference in profile shape (Fig. 5A). This is also reflected in the low standard deviation of the profiles averaged within each region (Fig. 5B), illustrating that this portion of the profile is similar along the entire study area. The influence of the variable offshore bathymetry on the average profile shape becomes apparent seaward of 8 m water depth, beyond 150 m offshore (Fig. 5A). Large changes were also measured on the backbeach.

Sediment samples obtained during calm weather conditions show that the sediment in the study area can be generally classified into three categories: well sorted medium sand, poorly sorted gravelly sand, and poorly sorted bi-modal sand and gravel (Table 1). Bi-modal distribution is defined here as a distribution with two peaks with the secondary peak having at least 30% magnitude of the primary peak. Considerable cross-shore variation in the grain size exists. In general, the backbeach and offshore sediment is composed of well- to moderately sorted medium sand. The berm crest and inner surf zone are composed of moderate to poorly sorted gravelly sand. The swash zone, moving dynamically with the tide fluctuation, is often composed of bi-modal sand and gravel (Table 1). Little alongshore variation in mean grain size exists between the five regions, consistent with the lack of alongshore variability in the average profile shape right at the shoreline (Fig. 5A). Although the sediment surface of the lower swash zone is often covered by gravel-sized particles as observed during the sampling, the mean grain size of the 5 cm-thick surface samples often does not convey the grain size distribution apparent on the sediment surface (i.e., the mean grain size

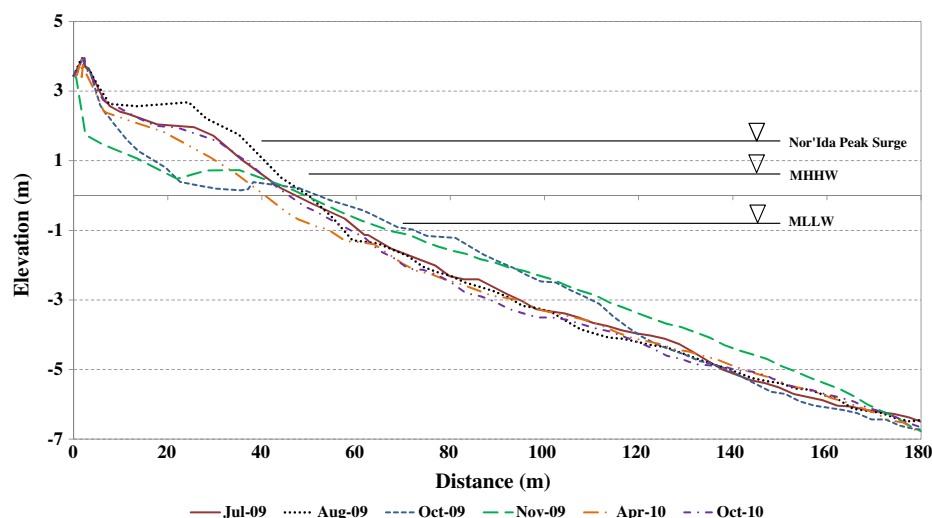


Fig. 4. Example profile RE N22 illustrating the absence of a sandbar throughout the study period. Elevation is referred to NAVD88. Mean Higher High Water (MHHW), Mean Lower Low Water (MLLW), and the peak Nor'Ida storm surge are indicated for reference.

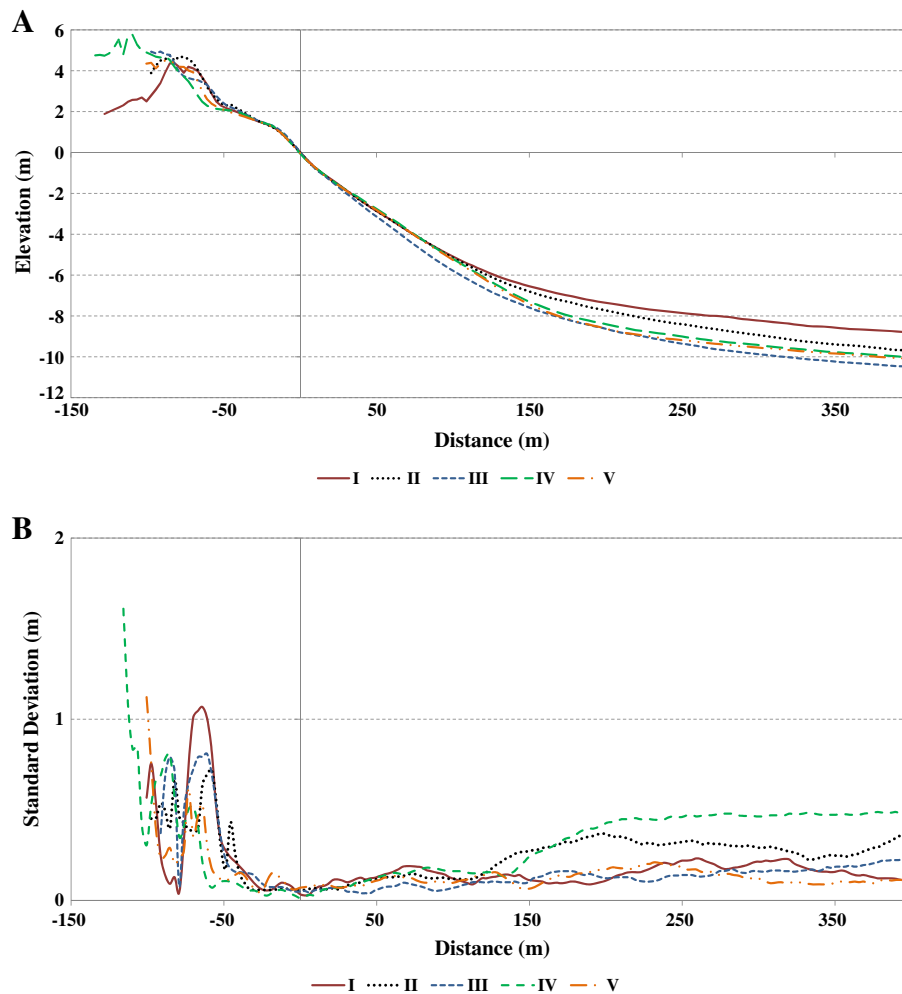


Fig. 5. A) Regionally averaged beach profiles. Note that the portion in the vicinity of the shoreline within the nearshore profile is similar for all five regions, diverging offshore due to the alongshore bathymetric variability. B) Standard deviation about the averaged beach profiles.

does not capture the bi-modal nature of the sediment, as the larger and smaller fractions average out).

#### 4.2. Cyclic beach morphodynamics

Dubois (1988) described the general seasonality of the Delaware beaches as having a wide, built-up summer profile and deflated, eroded winter profile. Similar seasonality was also identified in this study (Fig. 6). The majority of the sediment transported offshore during winter is deposited across the nearshore, mostly above the  $-4$  m elevation contour, but not in the form of a sandbar. Furthermore, the monthly beach profile data allow for examining seasonal changes at a shorter temporal scale, revealing cyclic storm and inter-storm beach morphology changes, as discussed in the following sections.

##### 4.2.1. Characteristics of three consecutive storms in 2009

The three storms exhibited different oceanographic conditions (Figs. 2, 7, and 8). The maximum significant wave height associated with each storm increased, although with varied dominant wave periods reported by NDBC 44009 wave buoy (Fig. 1A, circle with black dot). Waves associated with Hurricane Bill exhibited the longest wave period of the three storms indicative of the swell conditions associated with the distal passage of the hurricane (Fig. 7). The maximum wave height measured at the offshore wave buoy during the distal passage of Hurricane Bill was 3.56 m with a maximum wave period of 19 s. The dominant wave period oscillated between 5 and 15 s as the storm

waves approached the study area, indicative of a bi-modal spectrum (Fig. 7). Although initially bi-modal, the wave conditions during Hurricane Bill became better organized into long, swell-type waves with a dominant wave period ranging from 16 to 19 s, typical of distal passages of tropical cyclones (or energetic summer swell). An average wind velocity of nearly 5 m/s primarily directed offshore, measured at the NDBC 44009 buoy, indicating minimal direct influence of storm-generated winds. Tidal measurements suggest that little to no surge associated with Hurricane Bill, likely attributed to the distance of the storm (Fig. 8).

Although not the first winter “disturbance” in the study area in 2009, the October 18th winter storm was the first significant storm of the 2009 season, in terms of storm duration. The maximum wave height measured was approximately 5 m with a maximum dominant wave period of nearly 14 s. During the peak of the storm, the dominant wave period ranged mostly from 7 to 12 s. Wave conditions exceeding 4 m (or roughly three times the 4-year average) wave height lasted 23 h. The winds were primarily from the northeast with maximum wind velocity of 17 m/s. These onshore winds forced elevated water levels, with over a half-meter surge measured over eight tidal cycles (Fig. 8). The long-duration and height of the surge associated with the October 18th storm made this winter storm more damaging than the previous, brief storm a month earlier, during which negligible surge was measured (Fig. 2).

Nor’Ida is considered one of the most energetic storm events on record to impact the northeastern US coast, and impacted the Delaware

**Table 1**  
Cross-shore and longshore distribution of sediment characteristics.

Region	Location on profile	Mean (φ)	Size class	Std. dev (φ)	Sorting class	
I	Backbeach	1.20	Med sand	0.72	Moderately sorted	
	Berm	1.10	Med sand	0.56	Mod well sorted	
	Swash	1.66	Med sand	0.48	Well sorted	
	Lower swash	0.01	Coarse Sand	1.70	Poorly sorted	
	Shorebreak	-0.68	v coarse sand	2.32	V poorly sorted	
	SURF zone	1.17	Med sand	1.04	Poorly sorted	
	3 m water depth	2.00	Med sand	0.70	Mod well sorted	
	4.5 m water depth	1.84	Med sand	0.71	Mod sorted	
	6 m water depth	0.82	Coarse sand	1.03	Poorly sorted	
	II	Backbeach	1.61	Med sand	0.48	Well sorted
Berm		1.16	Med sand	0.55	Mod well sorted	
Swash		1.19	Med sand	0.41	Well sorted	
LL of swash		1.07	Med sand	1.21	Poorly sorted	
Shorebreak		1.53	Med sand	1.42	Poorly sorted	
Surf zone		2.04	Fine sand	0.71	Mod sorted	
3 m water depth		2.12	Fine sand	0.71	Mod sorted	
6 m water depth		1.43	Med sand	0.65	Mod well sorted	
III		Backbeach	1.36	Med sand	0.55	Mod well sorted
		Berm	1.60	Med sand	0.51	Mod well sorted
	Swash	1.23	Med sand	0.40	Well sorted	
	LL of swash	-0.36	v coarse sand	1.91	Poorly sorted	
	Shorebreak	-0.57	v coarse sand	2.18	V poorly sorted	
	Surf zone	1.15	Med sand	1.44	Poorly sorted	
	3 m water depth	1.85	Med sand	0.72	Mod sorted	
	6 m water depth	1.15	Med sand	0.78	Mod sorted	
	IV	Backbeach	1.57	Med sand	0.47	Well sorted
		Berm	1.37	Med sand	0.55	Mod well sorted
Swash		1.08	Med sand	0.49	Well sorted	
3 m water depth		1.61	Med sand	0.77	Mod sorted	
6 m water depth		1.01	Med sand	0.84	Mod sorted	
V	Backbeach	1.23	Med sand	0.53	Mod well sorted	
	Berm	1.00	Med sand	0.62	Mod well sorted	
	Swash	1.65	Med sand	0.45	Well sorted	
	3 m water depth	1.77	Med sand	0.72	Mod sorted	
	6 m water depth	1.57	Med sand	0.84	Mod sorted	

beaches from November 11th through the 14th of 2009, lasting over eight tidal cycles. The maximum significant wave height was 8.11 m with a maximum dominant wave period of nearly 14 s. During the five-day span of Nor'Ida, the energetic wave conditions exceeding 4 m wave height lasted 52 h, more than twice that of the October 18th storm. The maximum significant wave height of 8.11 m occurring around midnight on November 13th was more than twice that measured during Hurricane Bill and over 60% higher than that during the October 18th storm (Fig. 7). The dominant wave period ranged primarily from 11 to 14 s. Winds were persistently from the northeast during the five day period, with a maximum wind speed of 21 m/s.

The onshore winds elevated tidal levels nearly a meter over what was predicted (Fig. 8). Storm surge lasted over eight tidal cycles and was similar to the duration of October 18th storm. It is worth noting that the October 18th storm occurred during spring tides; and although the surge was less than during Nor'Ida, the overall peak water level was comparable (Fig. 8).

Wave propagation patterns under representative wave conditions were examined using CMS-WAVE model developed by Lin et al. (2008). Table 2 lists the input wave conditions. Roughly the 4-year average significant wave height, dominant wave period, and an easterly incident wave angle were used to represent a normal condition. The input wave condition representing Hurricane Bill was obtained by averaging the measured waves that were higher than 2.5 m (Fig. 7). The selection of averaging interval is subjective, aiming at providing a general representation of the peak of the storm. During the averaging interval, the wave period and incident wave angle remained fairly uniform, as reflected by the relatively small standard deviation (Table 2). The October winter storm was represented by averaging waves exceeding 3 m wave height (Fig. 7). For this averaging interval, again the wave period and incident wave angle, were fairly uniform. The model wave height input for Nor'Ida was represented by averaging waves higher than 3.5 m.

Wave propagation patterns under an average wave condition, Hurricane Bill, October winter storm, and Nor'Ida, as simulated by CMS-Wave model are considerably different, controlled by the interaction of the wave with the complicated bathymetry (Fig. 9). The modeled wave field under average condition is illustrated in Fig. 9A. Wave shoaling over the shallow water (southern part of the Delaware Bay ebb tidal delta) is apparent. Overall, the waves in the nearshore study area are fairly uniform under the average wave condition. The longer and higher Hurricane Bill swell waves interact with the shallow water much more noticeably than the average condition resulting in alongshore variation in nearshore (just before breaking) wave conditions (Fig. 9B). Refraction of the long wave over the shallow shoal (Fig. 1) is apparent, resulting in different wave angles along the shoreline (Fig. 9B). For this southerly approaching wave case, the incident wave angle is more oblique to the shoreline in the southern portion of the study area than in the northern portion. A general southward decreasing wave height was modeled, from approximately 2.2 m at the northern end to 1.8 m at the southern end of the study area, or a wave height decrease of 18%. For the shorter northerly approaching October 18th storm wave, incident wave angle remain largely constant along the studied shoreline. A general southward increasing wave height was modeled, from roughly 1.8 m at the northern end to 2.1 m at the southern end of the study area, or a southward wave-height increase of 17% (Fig. 9C). The high Nor'Ida wave approached the shoreline largely perpendicularly. Considerable wave-height variation along the shoreline was modeled, decreasing

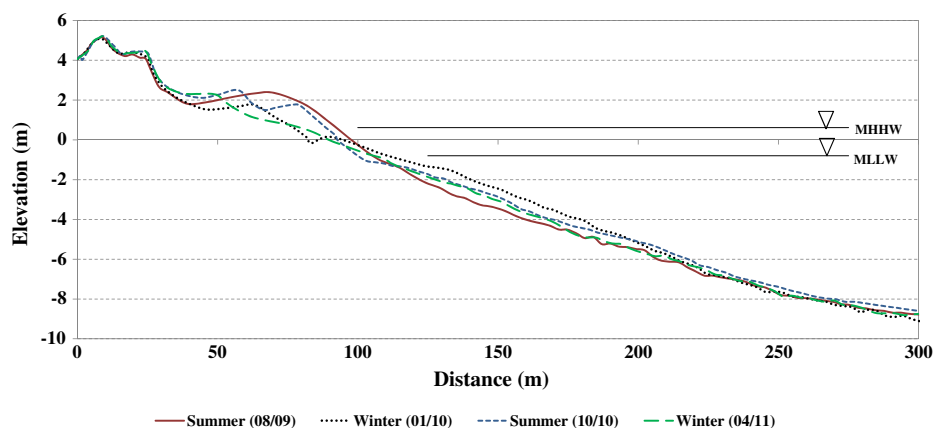


**Fig. 6.** Seasonality of the Delaware beaches illustrated by example profile, DE N15. Elevation is referred to NAVD88. Mean Higher High Water (MHHW) and Mean Lower Low Water (MLLW) are indicated for reference.

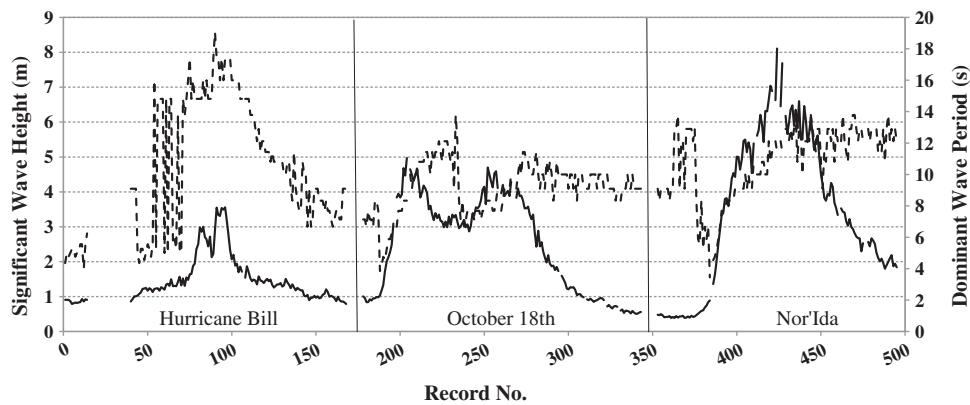


Fig. 7. Significant wave height (solid line) and dominant (peak) wave period (dashed line) for the three storms. Record number is arbitrary, carrying a unit of hour(s), for the convenience of illustrating the storm duration.

from south to north from roughly 4.0 m at the southern end to 3.5 m at the northern end, a southward wave height increase of 14% (Fig. 9D). The present wave modeling is qualitative and aims to illustrate regional scale variations of wave height and wave direction, which should provide valuable background information for the interpretation of morphology changes. Detailed and quantitative wave analysis is beyond the scope of this paper.

#### 4.2.2. Storm-induced beach morphology changes

The beach morphology and profile-volume changes resulting from the three different storms varied from beach accretion to erosion. The profile-volume change above the depth of closure following each of the three storms is shown in Fig. 10. Considerable alongshore variation occurred indicating the existence of longshore sediment transport gradients, likely related to the alongshore variation of wave height and wave direction as discussed above. It is beyond the scope of this paper to examine the details of longshore variation. The main goal here is to examine storm-induced profile changes in the cross-shore direction, i.e., beach cycles. Therefore, the following discussion is focused in a representative area with limited net change above closure depth, indicated in Fig. 10 with a box.

Cyclic beach-profile change is illustrated by a representative profile from approximately the middle of the study area at RE N22 for July 2009 through November 2009, showing both pre- and post-storm beach profiles (Fig. 11). Nomenclature used by the DNREC surveyors is utilized in this study for consistency and reproduction purposes. All beach-profile surveys extend to nearly 1 km offshore, however only the nearshore region is illustrated (for purposes of clarity). The July 2009

profile is representative of the typical summer, or built-up, beach conditions, with a 40 m-wide dry-beach from the base of the dune to the shoreline. The long-period swell waves generated by the distal passage of Hurricane Bill further elevated the dry-beach, depositing a 0.7-m thick layer of sediment on the berm crest and prograding the beach seaward. The source of the sediment appears to have derived from the nearshore, where erosion was measured between the shoreline and the  $-5$  m contour. The higher wave runup associated with the large swells (Roberts et al., 2010) generated during Hurricane Bill is likely responsible for the higher than typical elevation ( $>2$  m NAVD88) of beach aggradation.

The built-up summer beach profile was severely eroded following the October 18th winter storm (post-storm profile illustrated by the October 2009 survey line Fig. 11), with up to 2.5 m of vertical deflation from the dune edge to the shoreline. This beach/berm deflation is a typical characteristic of winter or post-storm beach morphology along the Delaware and adjacent coast, as well as other beaches. The shoreline (defined as zero NAVD88) remained stable as compared to the pre-storm position, while the majority of the eroded sediment deposited in the nearshore region as a layer of sediment up to 1 m thick between the 0 m and  $-4$  m NAVD88. The eroded sediment did not deposit offshore in the form of a sandbar along all the profiles.

Extreme wave conditions during the Nor'Ida storm overwhelmed the beach and dunes of 3–4 m height, with intense wave breaking over a wide beach and nearshore zone (Fig. 12). The surge and wave runup did not continuously overtop and inundate the dunes, however they did induce active dune scarping and avalanching that resulted in between 3 to 10 m of landward dune retreat across most of Delaware

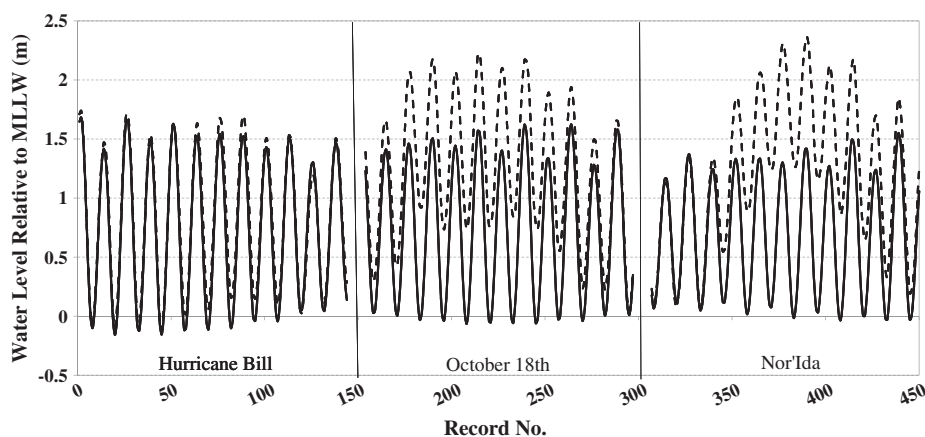


Fig. 8. Predicted (solid) and observed (dashed) water level relative to Mean Lower Low Water (MLLW) during the three consecutive storms, illustrating the associated storm surges.



**Table 2**

Input wave conditions for the schematic wave propagation modeling. Average wave conditions were used.  $\pm$  indicates one standard deviation about the mean.

	Normal condition	Hurricane Bill	October 18th storm	Nor'Ida
$H_{sig}$ (m)	1.5	2.96 $\pm$ 0.45	3.73 $\pm$ 0.53	5.51 $\pm$ 1.08
$T_p$ (s)	7.6	16.3 $\pm$ 1.3	9.4 $\pm$ 1.7	11.5 $\pm$ 1.3
Wave dir. (deg)	90	129.9 $\pm$ 1.8	71 $\pm$ 4	93 $\pm$ 7
Wind speed (m/s)	0	5.42 $\pm$ 1.52	130.2 $\pm$ 2.17	15.86 $\pm$ 3.24
Wind dir. (deg)	0	175 $\pm$ 49	57 $\pm$ 6	38 $\pm$ 8

coast. Following the passage of Nor'Ida, the shoreline remained fairly stable as compared to the pre-storm position, while the eroded beach and dune sediments were deposited in the nearshore as a nearly 1 m thick planar layer of sand, rather than as a sandbar, similar to the morphology change induced by the October 18th storm (Fig. 11). As a result of a deeper storm-wave base associated with the much larger waves, the eroded sediments from Nor'Ida were deposited in deeper water as compared to the typical winter storm, with sand accumulation between the 0 m and  $-6$  m contours.

The date of pre- and post-storm surveys is crucial to capturing the precise beach conditions and the exact temporal scale of beach cycle. For example, Fig. 13 shows pre- and post-storm photos of beach conditions in reference to the October 18th and Nor'Ida storms. Marked erosion occurred following the October 18th storm (upper right), however, considerable beach recovery was apparent prior to Nor'Ida (lower left). Because the beach profile data were collected (nearly) monthly, only one survey was conducted between the October 18th storm and Nor'Ida. The post-October 18th storm profile surveyed on October 20, 2009 is used to represent pre-Nor'Ida beach conditions (Fig. 11). The apparent beach recovery as illustrated in the photos taken on November 10th (Fig. 13), is not captured by the profile surveyed on October 20th (Fig. 11). In

other words, the magnitude of erosion following the Nor'Ida storm may be underrepresented due to the absence of beach profile data between the October 18th storm and Nor'Ida. In addition, the post-Nor'Ida beach profile data were collected two weeks following the peak of the storm, and therefore did not capture the full-extent of storm impact as post-storm recovery had already commenced (as discussed in the following sections).

#### 4.2.3. Pre- and post-Nor'Ida sediment properties

Within 48 h before and after the passage of Nor'Ida, sediment cores were obtained at three cross-shore locations at several alongshore transects (Fig. 3) to examine the detailed sedimentological characteristics associated with storm deposits on a MSG beach. The scheme of the sediment coring is illustrated in Fig. 13 (lower left, approximated by three x's). The morphologic locations of the cores from landward to seaward are backbeach, berm crest, and mid-swash (relative to the pre-Nor'Ida beach morphology). The pre-Nor'Ida cores represent the subsurface sediment distribution of a profile that has undergone considerable post-storm beach recovery (Fig. 13, lower left). The post-Nor'Ida cores represent the subsurface of a severely eroded and deflated beach profile (Fig. 13, lower right). Because the cores were obtained from similar cross-shore locations before and after Nor'Ida, the sediment characteristics associated with the erosion and deposition caused by Nor'Ida are obtained directly from comparing the cores.

Sediment erosion and deposition associated with Nor'Ida on the pre-storm backbeach are shown in Fig. 14. Cores RE-12 and RE-30 illustrate the pre- and post-Nor'Ida backbeach subsurface sediment composition, respectively. The dashed lines indicate the sedimentary layer contacts within the cores and the associated layers' grain size statistics. Overall, the meter-thick pre-Nor'Ida backbeach sediment is mostly well to moderately well-sorted medium sand, with a mean grain size ranging from 1.77 to 1.02  $\phi$  (0.29 to 0.49 mm) across the four layers identified (RE-12). In the post-Nor'Ida backbeach core (RE-30), the sediment

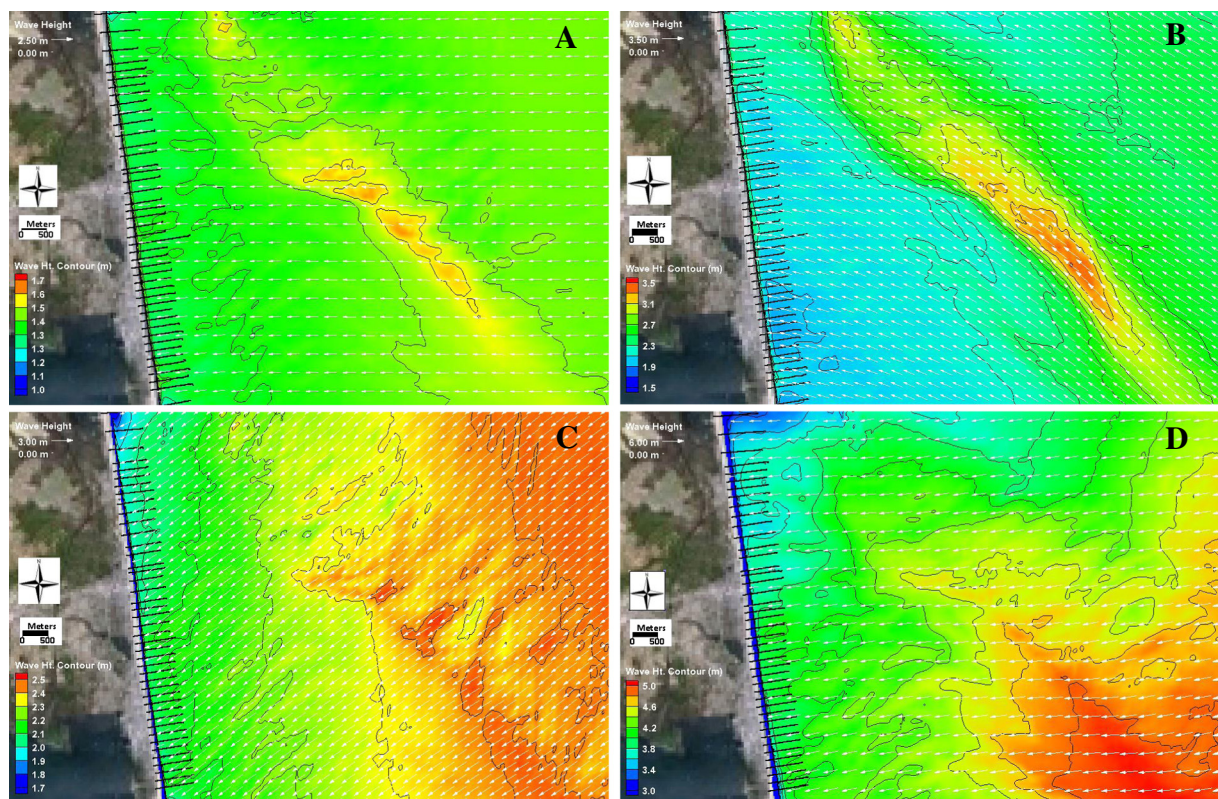


**Fig. 9.** CMS-Wave modeling results using averaged wave input parameters measured at NDBC 44099 to illustrate the nearshore wave field for A) typical or average conditions; B) Hurricane Bill; C) the winter storm during October 2009; and D) Nor'Ida.

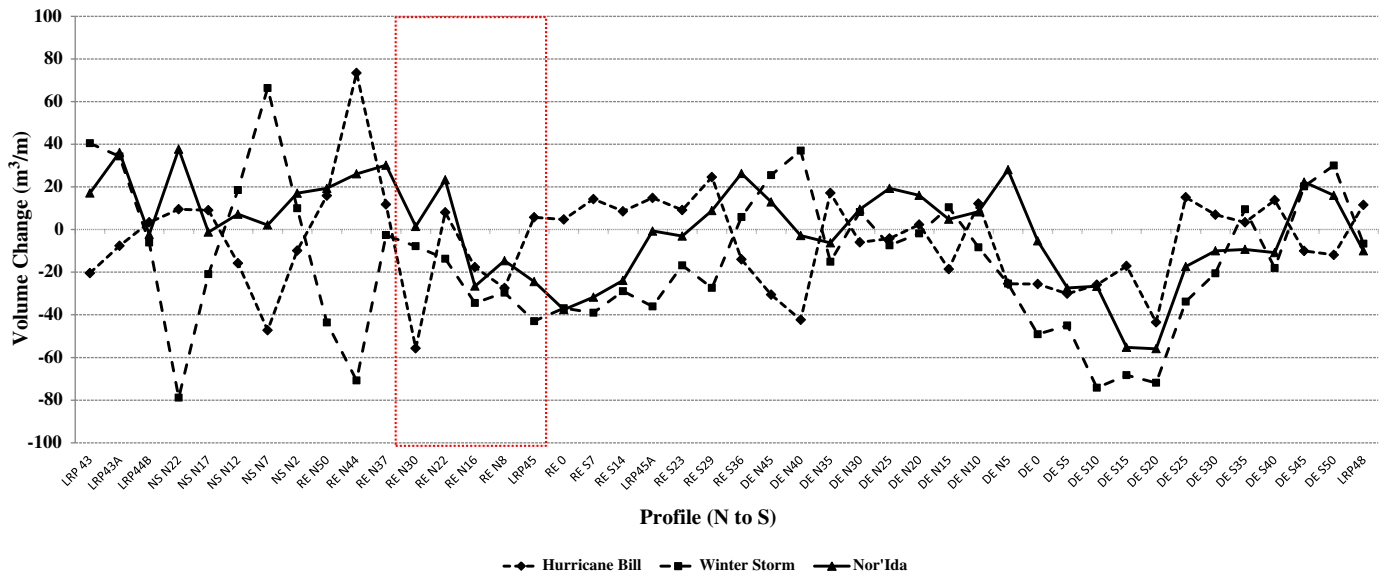


**Fig. 10.** Total volume change above the short-term depth of closure (determined by profile convergence during the study period) for the 46 beach profiles following the three consecutive storms, Hurricane Bill, October winter storm, and Nor'Ida. The red box indicates the focus area for discussion. (For interpretation of the references to color, the reader is referred to the web version of this article.)

layer between 78 cm and 117 cm is comparable to the pre-Nor'Ida well-sorted medium sand. However, the upper 78 cm of sediment was remarkably different from the pre-Nor'Ida well-sorted medium sand. The poorly sorted very coarse sand layer had a gravel/sand/mud (G/S/M) fraction ratio of 26/74/0. It is recognized that the actual elevation of the top of the backbeach core is not the same before and after the storm due to substantial erosion induced by Nor'Ida depleting this portion of the profile (as illustrated by the photos shown in Fig. 13). The above comparison was not based directly on the absolute elevation of the layers, but rather was based on the daily observations during the passage of the storm (for example, Fig. 12).

Cores obtained from the approximate cross-shore location of the pre-storm berm crest are shown in Fig. 15. The pre-Nor'Ida berm crest core (RE-11) was obtained under nearly "built-up" beach conditions. The top 30 cm was composed of poorly sorted medium sand with a G/S/M ratio of 11/89/0. From 30 to 110 cm, the sediment was composed of multiple layering of poorly sorted gravelly coarse sand. In the post-Nor'Ida core

(RE-31) taken at a similar location, the upper-most 6 cm thick layer was comprised of very poorly sorted pebbles. From 6 to 58.5 cm, the sediment is mostly moderately-well sorted to moderately sorted, medium to coarse sand. Again, the elevations at the top of the cores are different, because the pre-storm berm crest was completely eroded by Nor'Ida. Interestingly, except at the very surface covered by a layer of pebble lag, the post-Nor'Ida core illustrates improved sediment sorting, due to a decreased coarser fraction, at the pre-storm berm crest location (Fig. 15).

Both cores obtained at the cross-shore location of the pre-storm mid-swash zone region exhibited alternating layers of sand and gravel (Fig. 16). The top 25 cm of the pre-Nor'Ida core (RE-10) was composed of poorly-sorted coarse sand, with some gravel (~3%), overlying poorly-sorted gravelly sand. Overall, the core exhibits multiple layering of sand and gravelly sand (greater than 25% gravel), representing migrating swash zone driven by fluctuating tide water level. The top 11 cm-thick layer of sand in the post-Nor'Ida core (RE-32) taken at a similar location

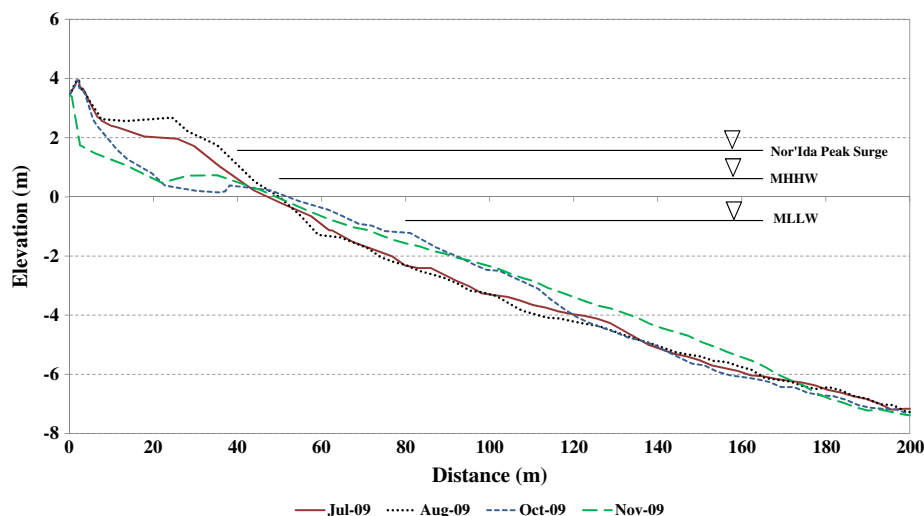


**Fig. 11.** Example beach profile, RE N22 + 12, from roughly the middle of the study area, illustrating time-sequenced beach profiles from 2009 to 2011. Elevation is referred to NAVD88. Mean Higher High Water (MHHW), Mean Lower Low Water (MLLW), and the peak Nor'Ida storm surge are indicated for reference.

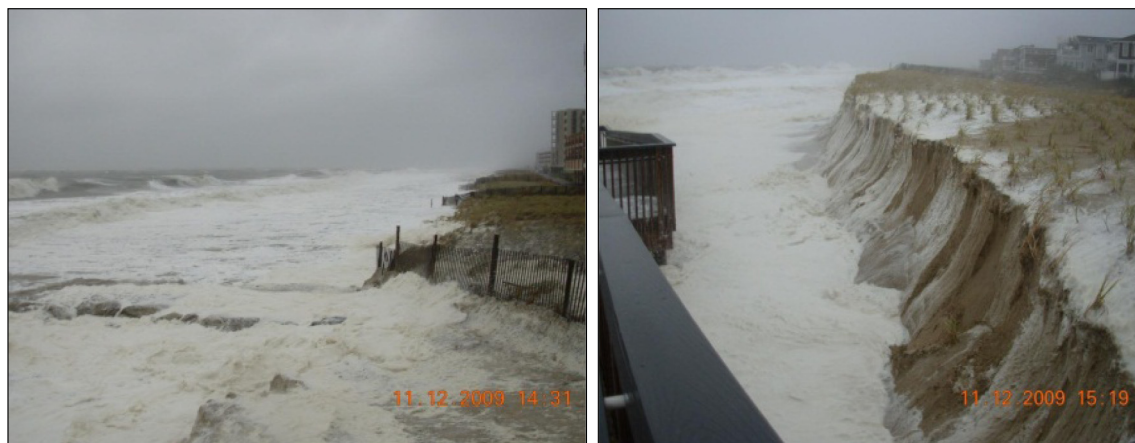


**Fig. 12.** Photos of the wide, energetic surf zone during Nor'Ida (left). The resultant dune avalanching and severe beach erosion is shown (right). The dunes in the left photo are more than 3 m high, serving as a qualitative reference for the breaking waves during Nor'Ida.

was composed of moderately well-sorted medium sand (only ~1% gravel) overlying a gravel lag (from 11 to 26 cm). The basal 30 cm of sand is similar to the post-Nor'Ida berm-crest core (Fig. 15), interpreted as improved sorting by storm processes. In contrast to the previous two sets of cores, the top elevations of the mid-swash zone cores are comparable. Almost all of the pre- and post-Nor'Ida beach profiles (e.g., Fig. 11) had a similar location and elevation of the shoreline (~0 m NAVD88), approximately where the mid-swash cores were obtained. Due to the dynamic nature of this zone under both normal and storm conditions, it is difficult to distinguish storm deposits from normal deposits.

#### 4.2.4. Short-term post-storm beach recovery

Rapid post-storm beach recovery (defined here as days to weeks) occurs as storm energy subsides. The beach recovery took the morphologic form of a developing ridge and runnel system along the entire studied beach. Fig. 17 (right) illustrates the initial development of a ridge and runnel system three days after the peak of Nor'Ida on November 16th. The ridge and runnel system cannot be identified just two days earlier from the photo obtained on November 14th during the first low-tide after the storm. Although the immediate post-storm recovery ridge and runnel had initiated (as discussed below), it had not yet migrated onshore to the subaerial portion of the beach (Fig. 17, upper



**Fig. 13.** Photos of pre- and post-October 18th storm beach conditions (top left and right, respectively). The same sand fence is circled in these top two photos for comparison. Photos of the pre- and post-Nor'Ida storm beach conditions (bottom left and right, respectively). The same building is indicated by arrows on the upper left, lower left, and lower right images for comparison. Note the remarkable beach recovery between October 18th and November 10th, 2009 (a couple days before the Nor'Ida storm). The crosses on the pre-Nor'Ida photo (lower left) denote the morphologic location of the sediment cores.

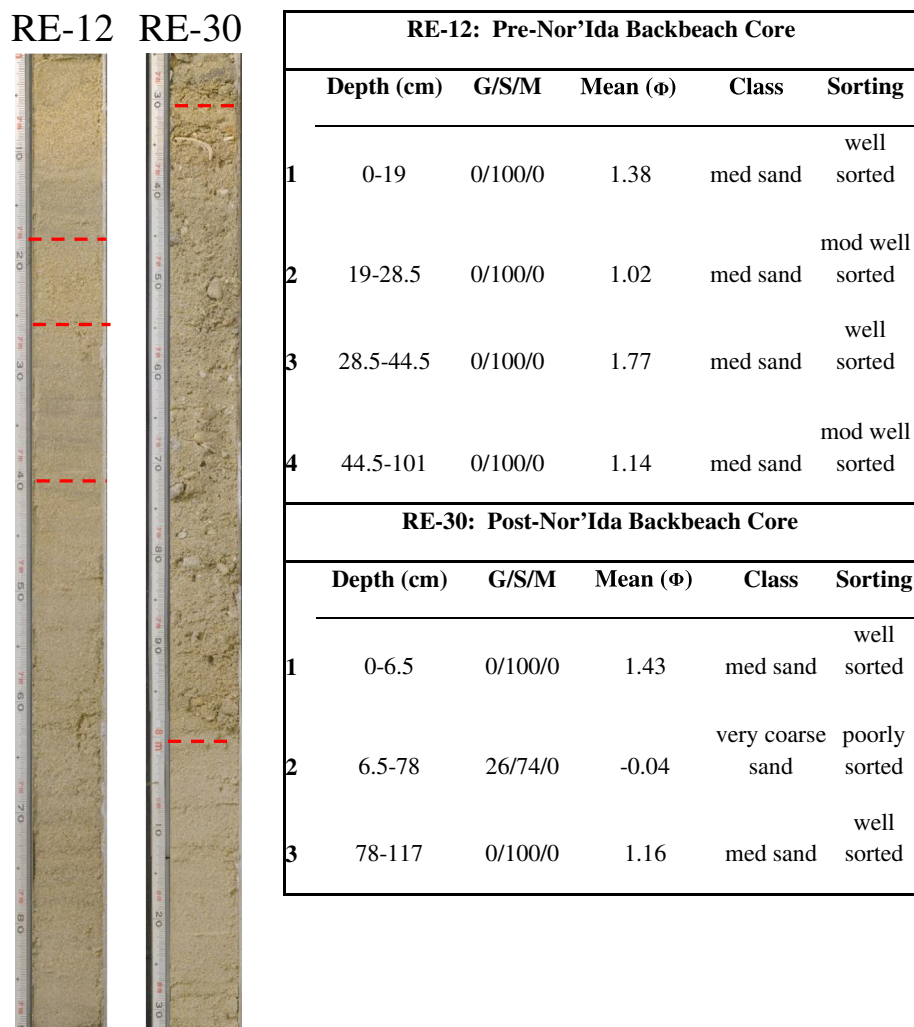


Fig. 14. Pre- and post-Nor'Ida backbeach sediment cores (left) with grain size statistics, classification, and gravel/sand/mud ratio (right) of each sedimentologically distinct layer (contacts shown by dashed lines). Layers are numbered from top to bottom.

right). The continued growth of the ridge and runnel is apparent in the photo obtained nearly one-month after Nor'Ida (Fig. 17, lower left).

This trend of immediate beach recovery is also illustrated by the profiles shown in Fig. 11. The post-October 18th storm survey was conducted two days after the storm impact (October 20th, 2009). The initial ridge and runnel system is captured by the October 20th survey, shown by the small 20 cm-high ridge located at approximately the 40 m cross-shore location. The post-Nor'Ida storm survey was conducted two weeks following the peak of the storm (December 1st, 2009). Thus, the ridge and runnel system illustrated by the Nov-09 data is better developed (with a cross-shore width of nearly 35 m). This explains the apparent accumulation of sediment on the backbeach when comparing the Oct-09 (post-October 18th storm/pre-Nor'Ida profile) and Nov-09 (post-Nor'Ida) profiles. The photos in combination with the survey data illustrate the rapid temporal scale at which beach recovery initiates along the Delaware beaches.

The short-term post-storm recovery morphology is illustrated at profile REN22 in Fig. 18. The post-October 18th storm short-term recovery was not captured by the beach surveys (illustrated by the photo in Fig. 13, lower left). The post-Nor'Ida ridge and runnel system continued to move landward and upwards in late December, building up the beach by transporting sediment from the nearshore to the subaerial beach (Fig. 17, lower left and Fig. 18). By late January 2010, two-months post-Nor'Ida, the ridge and runnel system had attached to the beach through onshore sediment transport infilling the runnel,

resulting in backbeach elevation gain. The short-term recovery continued through April 2010, with further backbeach elevation gain. It is worth noting that the above short-term storm recovery occurred in the middle of the winter season. Dune recovery did not occur naturally. In April 2010, artificial dune repair was conducted, explaining the apparent seaward dune progradation to the pre-Nor'Ida dune edge position.

Medium-term post-storm recovery (defined here as months to years) is shown at profile RE N22 in Fig. 19. Between April 2010 and April 2011, backbeach accretion continued with the development of a built-up beach, with a clearly defined berm crest. By July 2011, twenty months after Nor'Ida, nearly the entire beach profile recovered to its pre-storm July 2009 beach state. This particular medium-term beach recovery is also influenced by the relatively calm 2010–11 winter (Fig. 2). Although minor beach erosion occurred during the 2010–11 winter months (not shown in the figure), the relatively small intra-seasonal fluctuations in beach profile shape did not fundamentally alter the medium-term post-Nor'Ida beach recovery.

## 5. Discussion

### 5.1. Sedimentological characteristics of storm and post-storm deposits

The pre- and post-Nor'Ida sediment cores (Figs. 14, 15, and 16) illustrate the variability in sediment properties relating to built-up

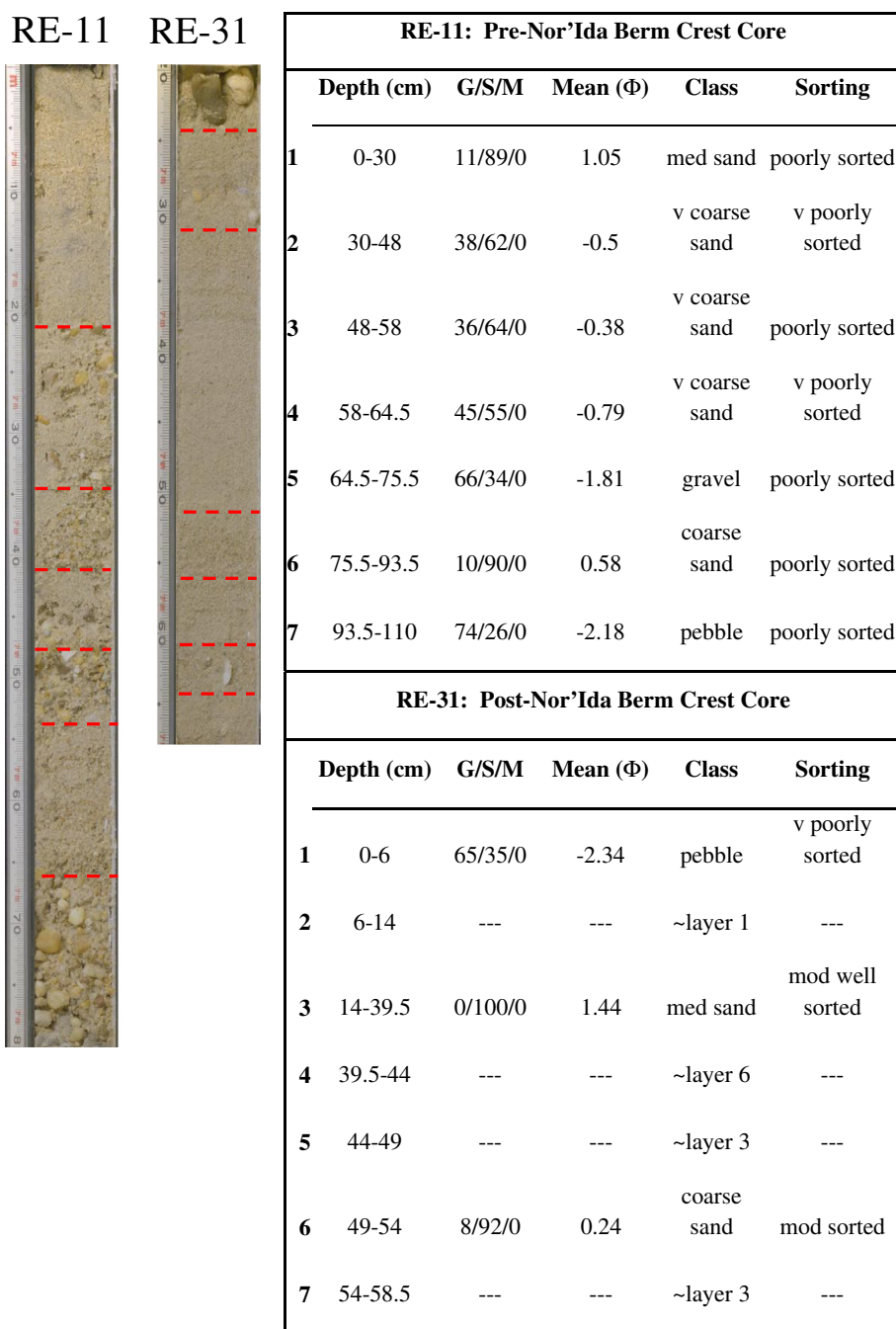


**Fig. 15.** Pre- and post-Nor'Ida berm crest cores (upper limit of swash) with grain size statistics, classification, and gravel/sand/mud ratio of each sedimentologically distinct layer (contacts shown by dashed lines). Layers are numbered from top to bottom.

(pre-storm) and depleted (post-storm) beach conditions. The built-up backbeach (Fig. 14, RE-12) was composed of well-sorted, to moderately well-sorted medium sand with little to no gravel, indicating that under non-stormy conditions gravel-sized sediment is not transported and deposited to the backbeach. Based on field observations of the backbeach during the storm, the nearly 72 cm-thick poorly sorted very coarse sand layer (G/S/M ratio of 26/74/0) in core RE-30 represents the Nor'Ida storm deposit. The sediment is interpreted to have been deposited in the upper portion of the wide storm swash zone (illustrated by the photo in Fig. 12, left). The storm deposit on the backbeach is associated with large waves during the elevated water levels occurring during the peak of the Nor'Ida storm. The upper-most 6 cm-thick layer of well-sorted medium sand with abundant heavy minerals is indicative

of the depositional conditions on the backbeach during the subsidence phase of the storm.

Multiple layers of poorly sorted, gravelly coarse sand are identified in the pre-Nor'Ida berm crest core (Fig. 15, RE-11). The poorly sorted medium sand from 0 to 30 cm is interpreted as post-October 18th storm beach recovery deposit. The layers from 30 to 93.5 cm are also interpreted as post-October 18th storm beach recovery deposits. During the early stages of post-storm beach recovery, the sediment surface was fairly low and subject to active swash-zone processes, allowing for deposition of sand, as well as gravel. As the elevation of the berm increases, for example above mean high tide level, only sand is deposited near the upper limit of swash runup, accounting for the top 30 cm of medium sand. The sandy gravel below 93.5 cm

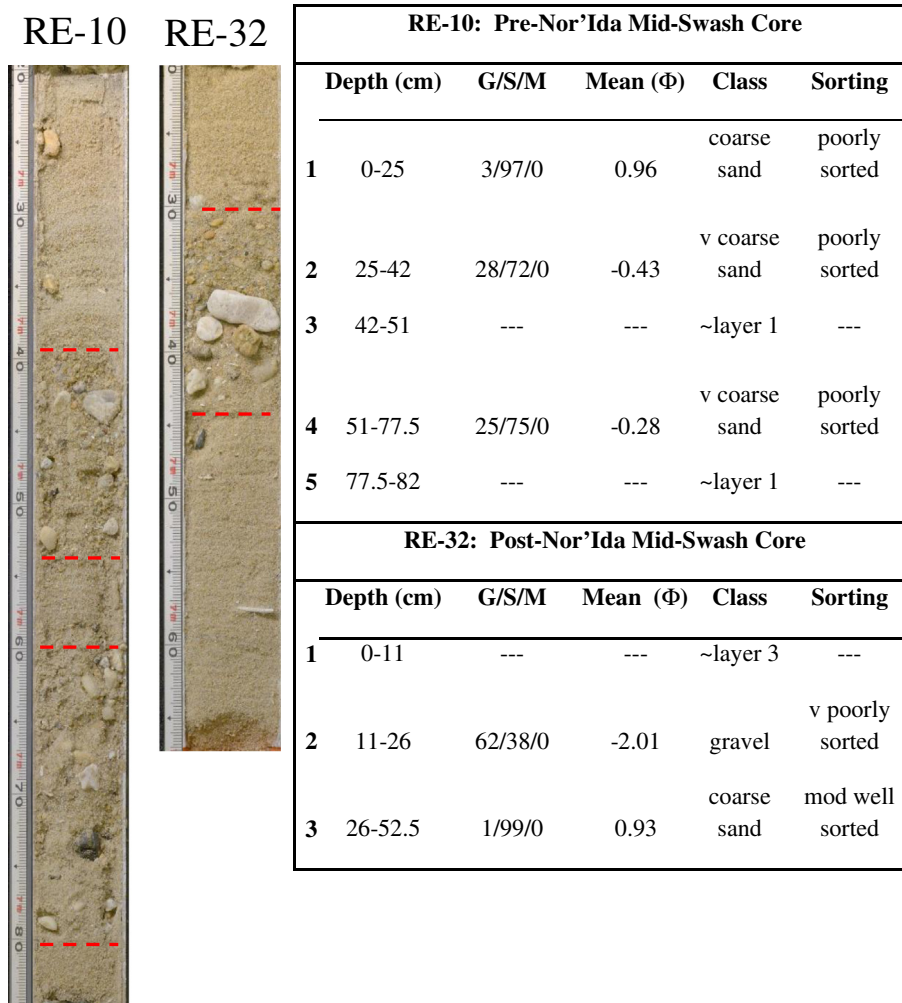


**Fig. 16.** Pre- and post-Nor'Ida mid-swash zone cores (swash) with grain size statistics, classification, and gravel/sand/mud ratio of each sedimentologically distinct layer (contacts shown by dashed lines). Layers are numbered from top to bottom.

is interpreted as the October 18th storm deposit. In the post-Nor'Ida core (RE-31) taken at approximately the same location, the uppermost 6 cm-thick layer is comprised of very poorly sorted pebbles, representing the lag deposit resulting from Nor'Ida. The remainder of the core (layers below) is mostly composed of moderately-well sorted to moderately sorted, medium to coarse sand, with little gravel identified (less than 10%). Despite the lack of gravel, this layer represents the Nor'Ida storm deposit, based on field observations during the storm. The post-Nor'Ida “berm crest” core was obtained on a section of the beach that was within the surf zone under elevated water level during the peak of Nor'Ida (Figs. 8 and 12). The lack of swash motion due to deep water may be the reason that no gravel was preserved in this layer of the storm deposit.

The alternating layers of sand and gravelly sand throughout the pre-Nor'Ida mid-swash zone core (Fig. 16, RE-10) represent active swash deposits likely modulated by tidal cycles. It is difficult to distinguish storm and non-storm deposits in the dynamic swash zone. The basal 30 cm of sand in the post-Nor'Ida mid-swash-zone core (RE-32) is interpreted as storm deposits, similar to sand layers (beneath the gravel lag) in the post-Nor'Ida berm-crest core (RE-31). The top 11 cm-thick layer of sand is interpreted as the immediate post-storm recovery overlying the Nor'Ida gravel lag (from 11 to 26 cm). On November 14th, 2009, as post-storm field data were being collected, the field and beach conditions were rapidly changing within hours. Fig. 20 (left) illustrates a photo of surface conditions at 12:32 (local time), with abundant gravel

lag covering the surface. The photo on the right was taken during the mid-swash-zone core retrieval, just 3 h later at 15:26 (local time). The surficial gravel lag observed at 12:32 was covered by 10 cm of sand at 15:26. This rapid change and large variation in sediment grain size indicates that selective transport and deposition occur concomitantly with the storm subsidence and post-storm recovery.

In summary, the storm deposit by Nor'Ida was characterized by a cross-shore variation in sediment grain size. In the storm upper swash zone (near the pre-storm dune edge), the Nor'Ida deposit was coarse, gravelly-sand (Fig. 14). While seaward of the storm swash zone (in this case equivalent to the pre-storm beach berm and foreshore), the Nor'Ida storm deposit was largely well-sorted medium sand beneath a layer of coarse lag probably deposited during the subsidence phase of the storm (Figs. 15 and 16). Therefore, the Nor'Ida storm deposit cannot be simply identified based on a layer of poorly-sorted coarse gravelly sediment. This also appears to be the case for the interpreted October 18th storm deposits. Gravelly sand or sandy gravel also occur in the active swash zone under normal conditions. The cross-shore distribution can be modulated by tidal water level fluctuations, complicating the interpretation of storm layers based on grain size.

### 5.2. Temporal scales of post-storm recovery

The widespread gravel lag deposit formed as the elevated storm water levels recede during the first low tide following Nor'Ida (Fig. 20,



**Fig. 17.** Photos showing the post-Nor'Ida beach recovery. One day after the Nor'Ida storm peak, a planar beach was covered in gravel at the first subsequent low tide (upper left). Within three days, the immediate beach recovery was in the morphologic form of a discontinuous ridge and runnel (right panel). Nearly one-month following the peak of Nor'Ida, the post-storm beach recovery morphology was in the onshore welding of a near-continuous ridge and runnel (bottom left).

left) serves as a sedimentological boundary separating the erosional and depositional phases of the storm. The immediate post-storm beach recovery was nearly concomitant with storm subsidence, as a sand layer deposited over the surficial pebble layer during the subsequent rising tide along with continued decreasing wave energy. This immediate storm recovery initiated in the ridge and runnel morphology.

In the short-term of weeks to months, the ridge and runnel system aggrades upwards while migrating onshore as beach recovery continues. The extensive presence of the ridge and runnel alongshore (Fig. 17) indicates that cross-shore processes dominate the immediate and short-term post-storm recovery. Five months following the Nor'Ida impact, the ridge and runnel attached to the beach, serving as the final

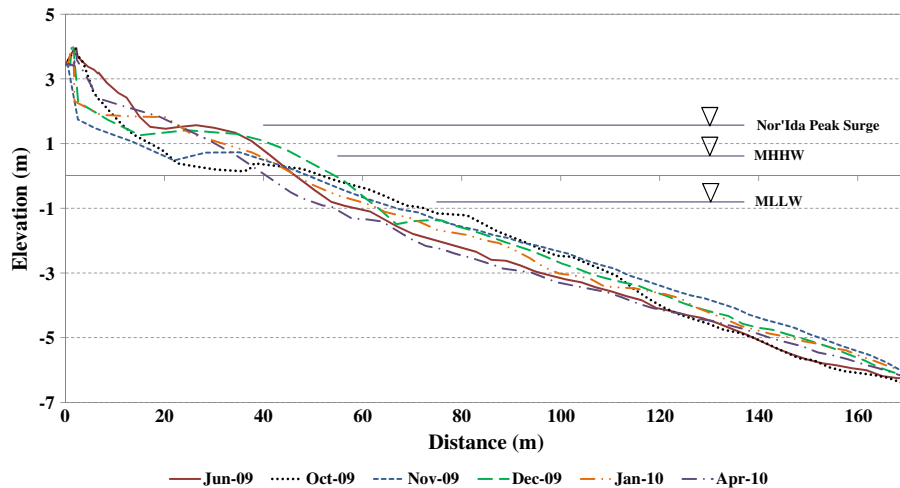


**Fig. 18.** Example beach profile RE N22 with time-sequenced profiles showing the short-term profile recovery following Nor'Ida (weeks to months). Elevation is referred to NAVD88. Mean Higher High Water (MHHW), Mean Lower Low Water (MLLW), and the peak Nor'Ida storm surge are indicated for reference.

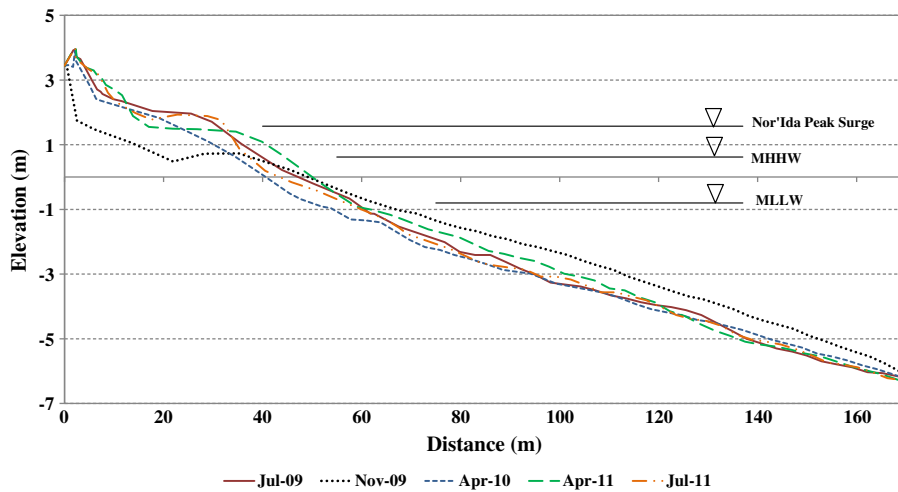


Fig. 19. Example beach profile RE N22 with time-sequenced profiles showing the medium-term post-storm recovery two years post-Nor'Ida (months to years). Elevation is referred to NAVD88. Mean Higher High Water (MHHW), Mean Lower Low Water (MLLW), and the peak Nor'Ida storm surge are indicated for reference.

morphologic stage of short-term recovery. Based on the data collected here, the time-scale of the ridge and runnel system appears to be on the order of months.

Barring no major subsequent storm impacts such as in this case, the medium-term recovery is characterized by continued backbeach aggradation and development of a clearly defined berm crest to a built-up beach profile. Two years post-Nor'Ida, the beach had essentially reached the pre-Nor'Ida conditions (Fig. 19). In addition, the Nor'Ida-deposited layer of sediments in the nearshore, between 1 and 6 m water depths, had migrated onshore almost entirely by July 2011, completing the beach cycle.

In summary, immediate post-storm recovery occurs as wave energy levels subside and return to normal conditions. Short-term recovery may be interrupted by subsequent storms, such as the recovery following the October 18th storm interrupted by the occurrence of Nor'Ida. Although the short-term recovery aids in beach progradation, it does not necessarily allow enough time to return to the full, built-up pre-storm conditions resulting from medium-term recovery, which requires extended periods of time (in this case two years) without a major storm impact. Therefore, the time-scale of the beach cycle is dynamic, controlled by storm energy levels and inter-storm duration, instead of simply seasonal.

### 5.3. The absence of a nearshore sandbar

Out of 740 profiles surveyed at 46 locations along the approximately 8 km stretch of the beach, over the two-year period, encompassing three different storms with various characteristics (including wave height, period, and surge), a nearshore sandbar never formed (Figs. 4 and 11). This suggests the existence of a dominant and persistent factor(s) preventing the formation of a nearshore bar under almost all wave conditions, ranging from steep storm waves to long-period swells. The lack of a sandbar under a wide range of wave conditions under which a bar often exists in many other places suggests that wave climate is not a determining factor in this case. In this section we explore several hypotheses for the lack of sandbar formation.

The overall relatively coarse mean grain size ranging from 1.5 to 0.5  $\phi$  (0.35 to 0.71 mm) and the heterogeneity of the sediment may play a role in the absence of a bar. Given the large temporal and spatial variations in gravel distribution, it is not possible to quantify the exact content of gravel within the sediment. Although the overall gravel concentration is not high, the gravel-sized particles tend to concentrate in the swash zone resulting in a steep foreshore during calm weather conditions. The reflective steep foreshore may play a role in the absence of a bar. Under stormy conditions, the gravel may have a substantial influence

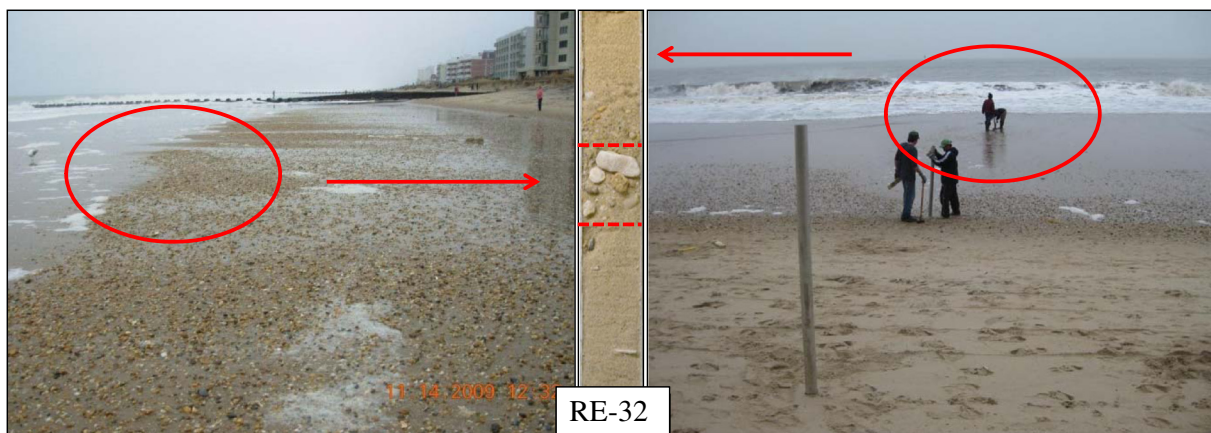


Fig. 20. Photos showing rapid temporal variation in surficial sediment after Nor'Ida. Left: Photo obtained during the first low-tide as Nor'Ida wave energy subsided showing surface conditions at 12:32 (local time) on 11/14/09 with abundant gravel covering the beach. Middle: Sediment core taken at the location shown in the right image (circle) shows a 10 cm layer of sand overlying a gravel layer. Right: Beach conditions during a rising tide at the time of post-Nor'Ida swash zone core retrieval (middle image) at 15:26 (local time) on 11/14/09. The circle on the left corresponds to the gravel layer in core RE-32 that was subsequently covered by a layer of sand during rising tide at the time of the core retrieval (circle on the right).



on sediment transport as illustrated by the wide-spread gravel lag distributed over the gentle storm beach. The gravel lag suggests that the very coarse grains may serve as an anchor for beach erosion to a certain depth. Exactly how the heterogeneity prevents the formation of a sandbar under all wave conditions, including storm events, is not directly apparent.

The absence of a sandbar is observed along the west-central Florida barrier island coast, in areas with a large persistent longshore transport gradient (Roberts et al., 2009; Roberts and Wang, 2012). After infusion of a large quantity of sediment, such as from beach nourishment, a bar might form but will not be maintained for an extended period of time. South of the study area, a regional divergent or nodal zone exists creating a northward longshore sediment transport gradient within the study area, as indicated by the large quantity of sediment bypassing at Indian River Inlet (Keshtpoor et al., 2013) and accumulation of sand at the northern terminus of the study area at Cape Henlopen. Detailed investigation of the potential influence of the longshore sediment transport gradients would be needed to address the absence of the sandbar, and are beyond the scope of this study. However, the divergence of longshore sediment transport associated with regional wave patterns may prevent a sand bar from being maintained. It does not explain why a storm sandbar was never formed.

#### 5.4. A storm-driven beach cycle model for non-barred mixed sand and gravel beaches

Classic description of beach cycles links seasonality to their beach states, such as a summer berm and winter bar profile (Fig. 21A). However, the MSG beaches of the Delaware coast persistently lack a sandbar; even after storms or high-energy events. Nevertheless,

the general seasonal beach cycles in terms of a summer berm profile or depleted winter profile exist. When examined at a temporal scale finer than seasonality, the beach cycles for the Delaware beaches are largely driven by storms and the duration of inter-storm recovery regardless of season. The frequency and intensity of the storms are related to seasonality, however, fundamentally the cycle is driven by storms and not the seasonality.

A modified beach cycle model for the non-barred Delaware MSG beaches is proposed in Fig. 21B. Following a storm or high-energy event, the subaerial beach erodes with offshore transport and deposition of the eroded berm sediment as a planar nearshore storm deposit. The seaward extent of the storm deposit is proportional to the storm energy; for example, the more energetic Nor'Ida storm deposited sediment much deeper than the October 18th storm. The eroded sediment is transported offshore and is distributed rather evenly throughout the nearshore region resulting in an overall mild beach slope. The deflated subaerial beach with the nearshore sediment deposit characterizes the "storm" profile. As the storm subsides, storm waves tend to become more organized into accretionary swell-type waves (Fig. 7), contributing to the immediate post-storm beach recovery. The initial beach recovery was in the form of a landward migrating and upward aggrading ridge and runnel system that served as the sediment pathway and morphologic mechanism for rebuilding the beach berm ("transitional" profile). Short and medium-term (months to years) beach recovery continues during calmer periods of relatively low-wave energy, resulting in the welding of the ridge and runnel to the beach and the foreshore slope becoming steep as the berm aggrades. The built-up beach berm and steep foreshore slope characterize the "recovery" profile. In contrast to onshore migration of the bar, the planar offshore storm deposit is eroded and transported onshore to build up the berm.

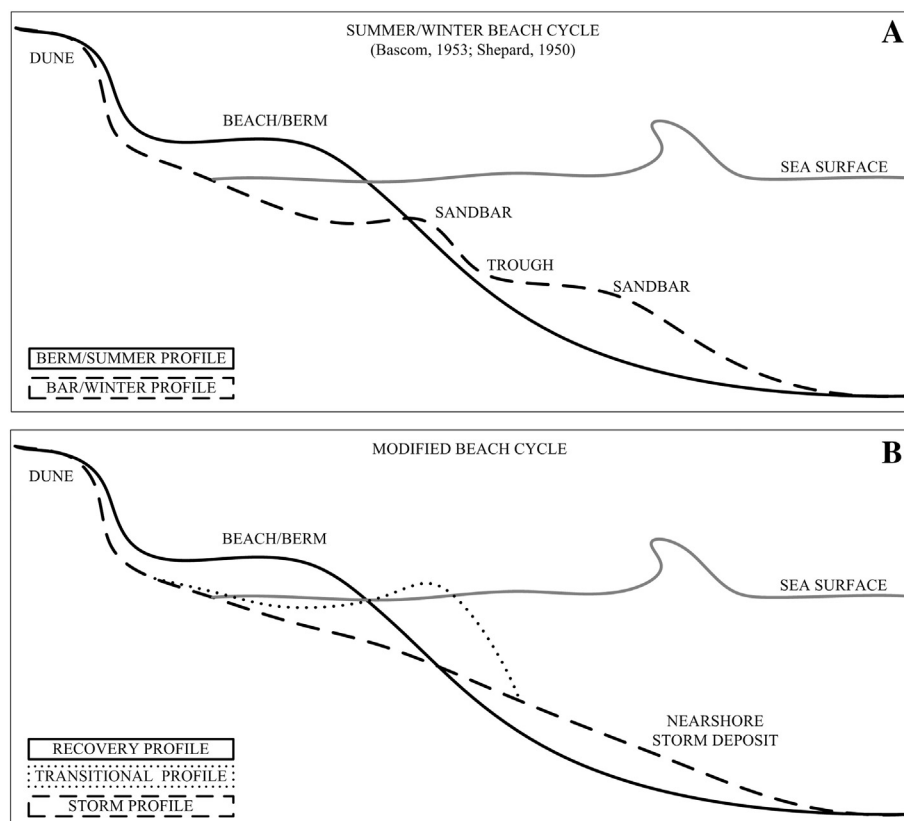


Fig. 21. A) Classic beach cycle model composed of bar-type (winter) and berm-type (summer) profiles (modified from Komar, 1998). B) Modified beach cycle model for a non-barred mixed sand and gravel beach illustrating the storm profile, transitional (initial recovery) profile, and the full recovery profile.

## 6. Conclusions

Based on (nearly) monthly beach profiles, sediment data, and observations made during the occurrence of three storms, the following conclusions are reached for the MSG beaches in Delaware:

- 1) The sediment characteristics of the storm deposit associated with Nor'Ida demonstrated substantial cross-shore variation ranging from coarser sandy-gravel and gravelly-sand within the storm swash zone (near the pre-storm dune edge) to well-sorted medium to coarse sand seaward of the storm swash zone. The Nor'Ida storm deposit along the MSG beaches in the study area could not be uniformly identified based on a layer of poorly-sorted coarse gravelly sediment, as the native swash zone is populated by mixed sediment with similar properties.
- 2) A sandbar did not form under any wave condition encountered during this study. Specific geologic conditions, including the mixed sediment grain size and potentially large longshore sediment transport gradient, may be attributed to the prevention of bar formation.
- 3) The initiation of post-storm recovery occurs during the subsiding phase of the storm, likely attributable to the reduction in wave height and steepness transitioning to accretionary post-storm swells.
- 4) Distinctive beach cycles in the morphological form of a built-up berm recovery profile and depleted nearly-planar storm profile are identified for the MSG Delaware coast. The transition between profile morphology is through a landward migrating and upward aggrading ridge and runnel system that served as the sediment pathway and morphologic mechanism for rebuilding the beach berm.
- 5) The time-scale of the beach cycles is dynamic, relating to the frequency and intensity of storm impact and duration of inter-storm recovery, instead of a simple and generalized seasonal cycle.
- 6) A beach cycle model, modified from the classic seasonal summer berm profile and winter bar profile, is developed for the Delaware MSG beaches reflecting a dynamic storm-driven time-scale and a planar non-barred post-storm beach.

## Acknowledgments

This study was jointly funded by the Delaware Department of Natural Resources and Environmental Control (DNREC), the University of South Florida (USF), and the University of Delaware. The authors would like to thank the USF graduate students and Kim McKenna (DNREC) who helped with the field data acquisition. We are very grateful to Anthony Pratt from DNREC, who provided some of the photos and many insightful discussions. The authors would also like to thank the thought-provoking and critically constructive comments and suggestions by two anonymous reviewers.

## References

Austin, M.J., Masselink, G., 2006. Observations of morphological change and sediment transport on a steep gravel beach. *Marine Geology* 229, 59–77.

Bascom, W.H., 1953. Characteristics of natural beaches. Proceedings of the 4th Coastal Engineering Conference. American Society of Civil Engineers, pp. 163–180.

Boczar-Karakiewicz, B., Davidson-Arnott, R.G.D., 1987. Nearshore bar formation by non-linear wave processes – a comparison of model results and field data. *Marine Geology* 77, 287–304.

Bodge, K.R., 1992. Representing equilibrium beach profiles with an exponential expression. *Journal of Coastal Research* 8 (1), 47–55.

Carter, R.W.G., Orford, J.D., 1993. The morphodynamics of coarse clastic beaches and barriers: a short- and long-term perspective. *Journal of Coastal Research Special Issue* 15, 158–179.

Claudino-Sales, V., Wang, P., Horwitz, M.H., 2008. Factors controlling the survival of coastal dunes during multiple hurricane impacts in 2004 and 2005: Santa Rosa barrier island, Florida. *Geomorphology* 95, 295–315.

Claudino-Sales, V., Wang, P., Horwitz, M.H., 2010. Effect of Hurricane Ivan on coastal dunes of Santa Rosa Barrier Island, Florida: characterized on the basis of pre- and post-storm LIDAR surveys. *Journal of Coastal Research* 26, 470–484.

Dalrymple, R.A., Mann, D.W., 1986. A coastal engineering assessment of Fenwick Island, Delaware. Technical Report No. CE-54. Univ. of Delaware, Newark, Delaware.

Dean, R.G., 1977. Equilibrium beach profiles: U.S. Atlantic and Gulf coasts. Department of Civil Engineering, Ocean Engineering Report No. 12. University of Delaware, Newark, Delaware.

Dolan, R., Davis, R.E., 1992. An intensity scale for Atlantic coast Northeast storms. *Journal of Coastal Research* 8 (4), 840–853.

Dubois, R.N., 1988. Seasonal changes in beach topography and beach volume in Delaware. *Marine Geology* 81, 79–96.

Figlus, J., Kobayashi, N., 2008. Inverse estimation of sand transport rates on nourished Delaware beaches. *Journal of Waterway, Port, Coastal, and Ocean Engineering* 134 (4), 218–225.

Forbes, D.L., Parkes, G.S., Manson, G.K., Ketch, L.A., 2004. Storms and shoreline retreat in the southern Gulf of St. Lawrence. *Marine Geology* 210, 169–204.

Gallagher, E.L., Elgar, S., Guza, R.T., 1998. Observations of sand bar evolution on a natural beach. *Journal of Geophysical Research* 103 (C2), 3,203–3,215.

Garringa, C.M., Dalrymple, R.A., 2002. Development of a long-term coastal management plan for the Delaware Atlantic coast. Res. Rep. No. CACR-02-04. Center for Applied Coastal Research, Univ. of Delaware, Newark, Del.

Greenwood, B., 2005. Bars. In: Schwartz, M.L. (Ed.), *Encyclopedia of Coastal Science*. Springer, The Netherlands, pp. 120–128.

Grosskopf, P.E., Bass, G.P., 2010. The Great Mid-Atlantic storm of 2009: 'Friday the 13th' storm impacts on Ocean City, Maryland. *Shore and Beach* 78 (2), 12–19.

Grunnet, N.M., Walstra, D.R., Ruessink, B.G., 2004. Process-based modeling of a shoreface nourishment. *Coastal Engineering* 51, 581–607.

Herrington, T.O., Miller, J.K., 2010. A comparison of methods used to calculate potential damage potential. *Shore and Beach* 78 (2), 20–25.

Hill, H.W., Kelley, J.T., Belknap, D.F., Dickson, S.M., 2004. The effects of storms and storm-generated currents on sand beaches in Southern Maine, USA. *Marine Geology* 210, 149–168.

Hoefel, F., Elgar, S., 2003. Wave-induced sediment transport and sandbar migration. *Science* 299, 1885–1887.

Holman, R.A., Bowen, A.J., 1982. Bars, bumps, and holes: models for generation of complex beach topography. *Journal of Geophysical Research* 87 (1), 457–468.

Holman, R.A., Sallenger, A.H., 1993. Sand bar generation: a discussion of the Duck experiment series. *Journal of Coastal Research Special Issue* 15, 76–92.

Horn, D.P., Li, L., 2006. Measurement and modeling of gravel beach groundwater response to wave run-up: effects on beach profile changes. *Journal of Coastal Research* 22 (5), 1241–1249.

Horn, D.P., Walton, S.M., 2007. Spatial and temporal variations of sediment size on a mixed sand and gravel beach. *Sedimentary Geology* 202 (3), 509–528.

Houser, C., Hamilton, S., 2009. Sensitivity of post-hurricane beach and dune recovery to event frequency. *Earth Surface Processes and Landforms* 34, 613–628.

Inman, D.L., Elwany, M.H., Jenkins, S.A., 1993. Shoreline and bar-berm profiles on ocean beaches. *Journal of Geophysical Research* 98 (C10), 18,181–18,199.

Ivamy, M.C., Kench, P.S., 2006. Hydrodynamics and morphological adjustment of a mixed sand and gravel beach, Torere, Bay of Plenty, New Zealand. *Marine Geology* 228, 137–152.

Jennings, R., Shulmeister, J., 2002. A field based classification scheme for gravel beaches. *Marine Geology* 186, 211–228.

Karunaathna, H., Horrillo-Caraballo, J.M., Ranasinghe, R., Short, A.D., Reeve, D.E., 2012. An analysis of the cross-shore beach morphodynamics of a sandy and a composite gravel beach. *Marine Geology* 299–302, 33–42.

Keshthpoor, M., Puleo, J.A., Gebert, J., Plant, N.G., 2013. Beach response to a sand bypassing system. *Coastal Engineering* 73, 28–42.

Komar, P.D., 1998. *Beach Processes and Sedimentation*, second edition. Prentice Hall, New Jersey.

Kraus, N.C., Larson, M., 1988. Beach profile change measured in the tank for large waves, 1956–1957 and 1962. Technical Report CERC-88-6. U.S. Army Corps of Engineers Waterways Experiment Station, Vicksburg, Mississippi.

Kraus, N.C., Smith, J.M., Sollitt, C.K., 1992. SUPERTANK Laboratory Data Collection Project. Proceedings of 23rd Coastal Engineering Conference. ASCE, New York, pp. 2191–2204.

Kriebel, D.L., Dean, R.G., 1993. Convolution method for time-dependent beach-profile response. *Journal of Waterway, Port, Coastal and Ocean Engineering* 119 (2), 204–226.

Lanan, G.A., Dalrymple, R.A., 1977. A Coastal Engineering Study of Indian River Inlet. University of Delaware, Delaware.

Larson, M., Kraus, N.C., 1989. SBEACH: numerical model for simulating storm-induced beach change. Technical Report CERC-89-9. U.S. Army Corps of Engineers, Vicksburg, Mississippi (266 pp.).

Larson, M., Kraus, N.C., 1994. Temporal and spatial scales of beach profile change, Duck, North Carolina. *Marine Geology* 117, 75–94.

Larson, M., Kraus, N.C., Sunumura, T., 1988. Beach profile change: morphology, transport rate, and numerical simulation. Proceedings of the 21st Coastal Engineering Conference. American Society of Civil Engineers, pp. 1295–1309.

Larson, M., Kraus, N.C., Wise, R.A., 1999. Equilibrium beach profiles under breaking and non-breaking waves. *Coastal Engineering* 36, 59–85.

Lee, G., Nicholls, R.J., Birkemeier, W.A., 1998. Storm-driven variability of the beach-nearshore profile at Duck, North Carolina, USA, 1981–1991. *Marine Geology* 148, 163–177.

Lemcke, M.D., Nelson, F.E., 2004. Cryogenic sediment-filled wedges, Northern Delaware, USA. *Permafrost and Periglacial Processes* 15, 319–326.

Lin, L., Demirebilek, Z., Mase, H., Zheng, J., Yamada, F., 2008. CMS-Wave: a nearshore spectral wave processes model for coastal inlets and navigation projects. US Army Corps of Engineers Engineer Research and Development Center Technical Report 08–13 (132 pp.).

Mason, T., Coates, T.T., 2001. Sediment transport processes on mixed beaches: a review for shoreline management. *Journal of Coastal Research* 17 (3), 645–657.

Masselink, G., Puleo, J.A., 2006. Sediment transport and morphological change in the swash zone. *Continental Shelf Research* 26, 661–680.

- McKenna, K.K., Ramsey, K.W., 2002. An evaluation of sand resources, Atlantic offshore, Delaware. Report of Investigations No. 62. Delaware Geological Survey.
- Morton, R.A., Sallenger, A.H., 2003. Morphological impacts of extreme storms on sandy beaches and barriers. *Journal of Coastal Research* 19 (3), 560–573.
- Morton, R.A., Paine, J.G., Gibeaut, J.C., 1994. Stages and durations of post-storm beach recovery, Southeastern Texas coast, U.S.A. *Journal of Coastal Research* 10 (4), 884–908.
- Munger, S., Kraus, N.C., 2010. Frequency of extreme storms based on beach erosion at northern Assateague Island, Maryland. *Shore and Beach* 78 (2), 3–11.
- Neal, A., Pontee, N.I., Pye, K., 2002. Internal structure of mixed-sand-and-gravel beach deposits revealed using ground-penetrating radar. *Sedimentology* 49, 789–804.
- NOAA Integrated Models of Coastal Relief (CRM), 2002. National Oceanic and Atmospheric Administration, National Geophysical Data Center. <<http://www.ngdc.noaa.gov/mgg/coastal/>>.
- NOAA WAVEWATCH III, 2013. National Weather Service, Environmental Modeling Center. <<http://polar.ncep.noaa.gov/waves/index2.shtml>>.
- Orford, J.D., Anthony, E.J., 2011. Extreme events and the morphodynamics of gravel-dominated coastal barriers: strengthening uncertain ground. *Marine Geology* 290, 41–45.
- Ozkan-Haller, H.T., Brundidge, S., 2007. Equilibrium beach profile concept for Delaware beaches. *Journal of Waterway, Port, Coastal and Ocean Engineering* 133 (2), 147–160.
- Plant, N.G., Holman, R.A., Freilich, M.H., Birkemeier, W.A., 1999. A simple model for interannual sandbar behavior. *Journal of Geophysical Research* 104 (7), 15,755–15,776.
- Pontee, N.I., Pye, K., Blott, S.J., 2004. Morphodynamic behaviour and sedimentary variation of mixed sand and gravel beach, Suffolk, UK. *Journal of Coastal Research* 20 (1), 256–276.
- Puleo, J.A., 2010. Estimating alongshore sediment transport and the nodal point location on the Delaware–Maryland coast. *Journal of Waterway, Port, Coastal, and Ocean Engineering* 3, 135–144.
- Ramsey, K.W., 1999. Beach sand textures from the Atlantic coast of Delaware. Open File Report No. 41. Delaware Geological Survey.
- Roberts, T.M., Wang, P., 2012. Four-year performance and associated controlling factors of several beach nourishment projects along three adjacent barrier islands, west-central Florida, USA. *Coastal Engineering* 70, 21–39.
- Roberts, T.M., Wang, P., Elko, N.A., 2009. Physical performance of beach nourishment projects along a microtidal low-energy coast, west-central Florida, USA. In: Mizuguchi, M., Sato, S. (Eds.), *Proceedings of Coastal Dynamics 2009*. Paper, no. 74. World Scientific, Tokyo, Japan.
- Roberts, T.M., Wang, P., Kraus, N.C., 2010. Limits of wave runup and corresponding beach-profile change from large-scale laboratory data. *Journal of Coastal Research* 26 (1), 184–198.
- Ruessink, B.G., Kroon, A., 1994. The behavior of a multiple bar system in the nearshore zone of Terschelling, the Netherlands: 1965–1993. *Marine Geology* 121, 187–197.
- Ruggiero, P., Kaminsky, G.M., Gelfenbaum, G., Voigt, B., 2005. Seasonal to interannual morphodynamics along a high-energy dissipative littoral cell. *Journal of Coastal Research* 21 (3), 553–578.
- Sallenger, A.H., Holman, R.A., Birkemeier, W.A., 1985. Storm-induced response of a nearshore-bar system. *Marine Geology* 64, 237–257.
- Shepard, F.P., 1950. Beach cycles in Southern California. Beach Erosion Board Technical Memo No. 20. U.S. Army Corps of Engineers.
- Stone, G.W., Liu, B., Pepper, D.A., Wang, P., 2004. The importance of extratropical and tropical cyclones on the short-term evolution of barrier islands along the northern Gulf of Mexico, USA. *Marine Geology* 210, 63–78.
- Turner, I.L., Masselink, G., 1998. Swash infiltration-exfiltration and sediment transport. *Journal of Geophysical Research* 103 (C13), 30,813–30,824.
- UDel/DE SGP (University of Delaware College of Earth, Ocean, and Environment and Delaware Sea Grant College Program), 2004. Striking a balance: a guide to coastal dynamics and beach management in Delaware, Report No. 40-07-01/04/08/06, Second edition. Univ. of Delaware, Newark, Delaware.
- USACE (United States Army Corps of Engineers), 1996. Rehoboth Beach/Dewey Beach Interim Feasibility Study: Final Feasibility Report and Final Environmental Impact Statement. United States Army Corps of Engineers, Philadelphia District, Philadelphia, Pennsylvania.
- van Duin, M.J.P., Wiersma, N.R., Walstra, D.J.R., van Rijn, L.C., Stive, M.J.F., 2004. Nourishing the shoreface: observations and hindcasting of the Egmond case, the Netherlands. *Coastal Engineering* 51, 813–837.
- Wang, P., Horwitz, M.H., 2007. Erosional and depositional characteristics of regional overwash deposits caused by multiple hurricanes. *Sedimentology* 54, 545–564.
- Wang, P., Kirby, J.H., Haber, J.D., Horwitz, M.H., Knorr, P.O., Krock, J.R., 2006. Morphological and sedimentological impacts of Hurricane Ivan and immediate post-storm beach recovery along the Northwestern Florida barrier-island coasts. *Journal of Coastal Research* 22 (6), 1382–1402.
- Wentworth, C.K., 1922. A scale of grade and class terms for clastic sediments. *Journal of Geology* 30 (5), 377–392.
- Wright, L.D., Short, A.D., 1984. Morphodynamic variability of surf zones and beaches: a synthesis. *Marine Geology* 56, 93–118.